AD-A044 567 UNITED TECHNOLOGIES RESEARCH CENTER EAST HARTFORD CONN F/G 20/8
ROTATIONAL POPULATION TRANSFER IN HF.(U)
AUG 77 J J HINCHEN, R H HOBBS F44620-76-C-0112
UNCLASSIFIED UTRC/R77-952595-1 AFOSR-TR-77-1202 NL

1 OF 1
AD
AD44 567

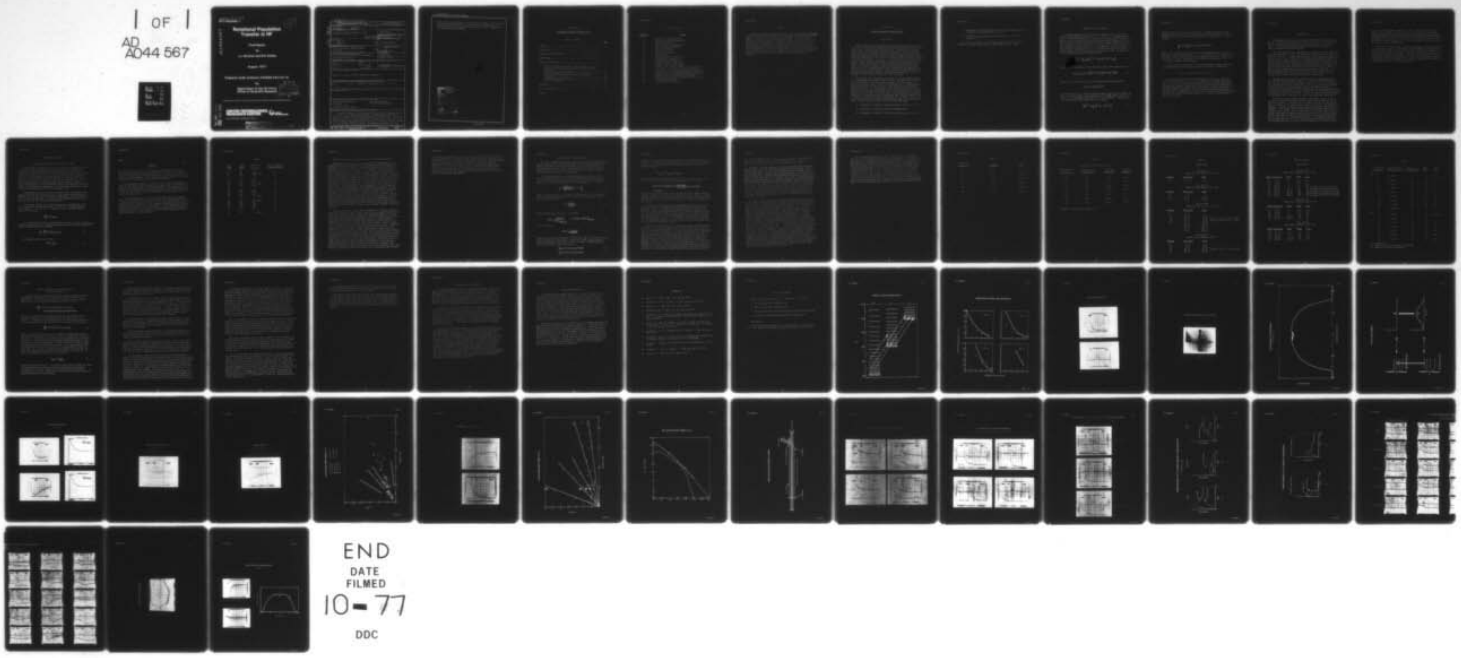

END
DATE
FILMED
10-77
DDC

R77-952595-1

Rotational Population Transfer in HF

Final Report

by

J.J. Hinchen and R.H. Hobbs

August 1977

Prepared under Contract F44620-76-C-0112

for

Department of the Air Force
Office of Scientific Research

UNITED TECHNOLOGIES RESEARCH CENTER

UNITED TECHNOLOGIES

EAST HARTFORD, CONNECTICUT 06108

77-09-2-1

UNCLASSIFIED

SECURITY CLASSIFICATION OF THIS PAGE (When Data Entered)

REPORT DOCUMENTATION PAGE	READ INSTRUCTIONS BEFORE COMPLETING FORM
1. REPORT NUMBER: AFOSR-TR-77-1292	2. GOVT ACCESSION NO. / 3. RECIPIENT'S CATALOG NUMBER
4. TITLE (and Subtitle): Rotational Population Transfer in HF.	5. TYPE OF REPORT & PERIOD COVERED: Final Report, May 1, 1976-August 31, 1977
	6. PERFORMING ORG. REPORT NUMBER: R77-952595-1
7. AUTHOR(s): J. J. Hinchen, R. H. Hobbs	8. CONTRACT OR GRANT NUMBER(s): F44620-76-C-0112
9. PERFORMING ORGANIZATION NAME AND ADDRESS: United Technologies Research Center, Silver Lane, East Hartford, Connecticut 06108	10. PROGRAM ELEMENT, PROJECT, TASK AREA & WORK UNIT NUMBERS: 2303/B1 61102F
11. CONTROLLING OFFICE NAME AND ADDRESS: Air Force Office of Scientific Research/NC, Bolling Air Force Base, Washington, D.C. 20332	12. REPORT DATE: August 30, 1977
	13. NUMBER OF PAGES: 53
14. MONITORING AGENCY NAME & ADDRESS(if different from Controlling Office)	15. SECURITY CLASS. (of this report): Unclassified
	15a. DECLASSIFICATION DOWNGRADING SCHEDULE

16. DISTRIBUTION STATEMENT (of this Report)

Approved for public release; distribution unlimited.

17. DISTRIBUTION STATEMENT (of the abstract entered in Block 20, if different from Report)

Final rept. 1 May 76-31 Aug 77

18. SUPPLEMENTARY NOTES

19. KEY WORDS (Continue on reverse side if necessary and identify by block number)

HF Rotational Relaxation
HF Lasing
Rotational Lasing
Collisional Energy Transfer
Far Infrared Lasing
Velocity Cross Relaxation

20. ABSTRACT (Continue on reverse side if necessary and identify by block number)

Population transfer in HF was measured by an IR double resonance experiment which uses HF pump and probe lasers. In three kinds of experiments populations pumped to a specific rotational level were followed: out of the pumped level, to the levels above, and to the levels below. The rates of loss from the pumped level and transfer to the lower levels were strongly affected by lasing between rotational levels. Measurements were made of gain and laser intensity and that information was incorporated into a kinetic rate

DD FORM 1 JAN 73 1473 EDITION OF 1 NOV 65 IS OBSOLETE

409252

UNCLASSIFIED

model to assess contributions to the total transfer rates. The collisional contributions are compared with linewidth data. Information was also obtained on population transfer rates for velocity cross relaxation and for vibration-rotation transfer.

Rotational Population Transfer in HF

TABLE OF CONTENTS

LIST OF FIGURES

ABSTRACT

Population transfer in HF was measured by an IR double resonance experiment which uses HF pump and probe lasers. In three kinds of experiments populations pumped to a specific rotational level were followed: out of the pumped level, to the levels above, and to the levels below. The rates of loss from the pumped level and transfer to the lower levels were strongly affected by lasing between rotational levels. Measurements were made of gain and laser intensity and that information was incorporated into a kinetic rate model to assess contributions to the total transfer rates. The collisional contributions are compared with linewidth data. Information was also obtained on population transfer rates for velocity cross relaxation and for vibration-rotation transfer.

Rotational Population Transfer in HF

INTRODUCTION

Chemical reactions between hydrogen and fluorine are used to pump excited states for HF lasers and are capable of populating high vibrational levels in the range of v = 3-7 and high rotational levels. Populations in high rotational levels may relax towards a Boltzmann distribution through collisonal energy transfer or by lasing on transitions between rotational energy levels. Rotational relaxation effects have recently been included in computer modeling of HF laser performance. Hall (Ref. 1) considered rotational lasing in addition to collisional relaxation in his model. We have previously reported (Ref. 2) studies of the collisional relaxation rates using I.R. double resonance techniques. Several authors (Ref. 3) have observed lasing between rotational levels of HF formed in reactions between F atoms and H_2. Skribanowitz and coworkers (Ref. 4) have described rotational lasing in HF gas samples pumped by radiation from a pulsed HF laser. The report herein describes IR double resonance measurements of population transfer between rotational levels of HF by both collisional energy exchange and rotational lasing.

The infrared double resonance technique for following rotational populations uses absorption of radiation from a pulsed laser operating on a single v(1-0) vibrational transition to pump population in an HF gas sample to a specific rotational J level in the v = 1 vibrational level. Collisional processes then redistribute this population among other rotational and other vibrational levels. A CW probe laser is used to monitor the rate of loss of population from the pumped rotational level or the rate of arrival of population in one of the other rotational levels. This is manifested as a temporal variation in the absorption of the CW radiation after the pulse laser fires. A diagram illustrating the types of experiments done is shown in Fig. 1. The pulse laser (denoted by the dashed line) populates level J and the CW probe laser is tuned to transitions A-E for the following experiments:

(A) Measurement of transfer to higher rotational levels, $\Delta J = 1, 2, \ldots$.

(B) Measurement of population loss from the pumped level.

(C) Measurement of transfer to lower rotational levels, $\Delta J = -1, -2, \ldots$.

(D) Measurement of combined population loss from the pumped level and filling in of the depleted level in v = 0.

(E) Observation of V-R population transfer from v = 1 to high J levels of v = 0.

In addition, information on momentum exchange between HF molecules is obtained by frequency tuning narrow linewidth pump and probe lasers.

SUMMARY OF PREVIOUS RESULTS

Rotational population transfer from J to higher levels (J + ΔJ) was measured after populating each of J2, J3, J4, J5 of v = 1 in separate experiments. After each of these levels was populated several higher levels were probed to follow the population transfer rate as the system approached equilibrium. Analysis of the results produced a general equation that provides for the description of rotational rates with a single rate constant. The results are completely described in Ref. 2. In development of the rate model and computer simulation, deactivation of the v = 1 HF was assumed to occur mainly through binary collisions with ground state molecules. With that assumption the rate equations governing the process were:

$$\frac{d}{dt} n_j^{v=1} = \sum_{i \neq j,k,l} \left(n_k^{v=0} n_i^{v=1} K_{ijkl} - n_k^{v=0} n_j^{v=1} K_{jikl} \right) \tag{1}$$

where n_j is the population in the vibrational state v and rotational level j,

$$K_{ijkl} = K_o \bar{n}_j \bar{n}_l e^{-\alpha \left| \left(E_j^{v=1} - E_i^{v=1} \right) + \left(E_l^{v=0} - E_k^{v=0} \right) \right| / kT} \tag{2}$$

where K_o and α are constants. $\bar{n}_j$ is the normalized Boltzmann population

$$\bar{n}_j = (2j+1) N^v(T) e^{-E_j^v / kT} . \tag{3}$$

This definition of K_{ijkl} satisfies detailed balance explicitly and assumes the rate to be proportional to the exponential of the energy defect in the collision (i.e. to the energy transferred to or from translation). Summing Eq. 1 over the unobserved ground state levels one obtains

$$\frac{d}{dt} n_j^{v=1} = P \sum_{i \neq j} \left(n_i^{v=1} K_{ij} - n_j^{v=1} K_{ji} \right) . \tag{4}$$

Using this model of the rate constant (Eq. 2) a computer simulation of the experiment was carried out -- including terms in the rate equation to describe the pumping pulse and the velocity redistribution. Dropping the v = 1 superscripts,

$$\frac{d}{dt} n_j = P \sum_{i \neq j} \left(n_i K_{ij} - n_j K_{ji} \right) + \eta_j - \beta n_j P \qquad (5)$$

where η_j is the pumping rate into level j from the pump pulse and β is the loss rate due to velocity redistribution ($\beta \sim 3 \times 10^5$ sec^{-1} $torr^{-1}$). The pump pulse was taken to have a zero rise time and an exponential decay with a characteristic time of 100 nsec. The population of rotational levels from J = 0 to J = 10 were included in the simulation.

Figure 2 presents the results of this simulation which compare reasonably to the experimental transfer rates using the two constants in the model:

$$K_o = 2.0 \times 10^8 \text{ sec}^{-1} \text{ torr}^{-1} \text{ and } \alpha = 1 . \qquad (6)$$

Previous work was devoted almost exclusively to the study of transfer from J to higher levels (J + ΔJ). A few observations of signals for transfer from J down to (J - ΔJ) showed these transitions to be extremely fast and we concluded that shortened pumping pulses would be needed for such measurements. The present program was aimed at making measurements of these "down" rates and also measurements of population loss from the level pumped using shortened pumping pulses. Subsequent observations showed that the fast rates were strongly influenced by lasing on rotational transitions. Studies of such lasing was added to the program.

EXPERIMENTAL

The apparatus for IR double resonance experiments has been described in Ref. 2. In essence it consists of two lasers, one of which is pulsed and the radiation used to pump populations in an HF gas sample to a specific V, J level. A second laser furnishes CW radiation for probing individual v, J levels to determine population transfer.

The HF gas absorption cell was made from a Kel-F tube 40 cm in length with an internal diameter of 12 mm. Calcium fluoride windows were held on each end with Kel-F wax. The two laser beams were made colinear and passed through the long axis of the cell. Diameters of both pulsed and CW beams were about 3 mm. The probe laser radiates a single P_{2-1} wavelength CW beam and operates on a single transverse cavity mode and can be tuned over about 350 MHz with a linewidth of about 10-30 MHz. Variation in the intensity of the CW laser due to absorption was monitored with a GeAu ($77^{o}K$) detector which had a sensitive area of 5 mm in diameter so that the entire CW beam was intercepted. A 1/4 meter spectrometer was placed before the detector as an optical filter. Detector signals were fed into an oscilloscope amplifier (Tektronix 7A15A) and the overall system rise time was less than 10 nanoseconds.

The pump laser is a multipin, transverse flow, pulsed discharge type that produces single wavelength radiation. Single P_{1-0} wavelength pulses of 0.1μ sec duration (FWHM) at 20 pps each contain about 0.03-0.05 mJ of energy. For investigating very fast transitions, such as J - ΔJ, the pulse length was shortened to avoid influencing signal shape by the pumping function. A Lithium Niobate polarizing "Q" switch (Lasermetrics, Inc.) was added external to the pulse laser optical cavity for this purpose. By this means, pulses could be shortened to about 40 nsec (FWHM). In Fig. 3 oscilloscope traces are shown for the natural pulse (top trace) and for a Q switched pulse (bottom trace).

The frequency of the pumping radiation, with respect to line center, is an important consideration because the probe laser must be tuned to coincide with this frequency. It was reported by Goldhar et al (Ref. 5) that the frequency of HF pulse laser ranges within 70 MHz of line center. We examined the frequency of content of the laser pulse using a AuGe detector and a spectrum analyzer. The frequency content exhibited over a five second period was within a range of about 40 MHz. This is illustrated in the picture shown in Fig. 4. No additional higher frequencies were found as far as 500 MHz. This evidence suggests that the pulse laser is operating on only a single longitudinal mode and all other modes are clustered within 40 MHz. The location of this frequency range with respect to line center was placed by observing the variation in signal amplitude for absorption of the CW radiation as the CW probe laser

was tuned over the Doppler linewidth. In Fig. 5, the CW laser output is shown as the frequency was varied during the double resonance measurement. The retracing near line center was obtained by constantly tuning for maximum absorption signal. This set the probe laser within a range of 50 MHz distributed ±25 MHz of line center. At other times we observed the range to remain at 50 MHz but to be displaced 20-30 MHz from line center. These results are in accord with Goldhar's observations.

The effects of narrow laser linewidths on the double resonance experiment is illustrated in Fig. 6. Since the pulse laser operates at line center only molecules from a small section of the velocity distribution are pumped and in order to interact with this velocity class, the CW laser must be tuned to the same frequency as the pulsed output. The tunability of the CW probe laser also made it possible to pump molecules in one velocity range and by suitable tuning measure the time for arrival in a different range and thus obtain collisional cross sections for velocity relaxation.

RESULTS AND DISCUSSION

Rotational Transfer Rates From J Down To (J-ΔJ)

A large number of experiments were run to look at the transition rates of populations to lower rotational levels. These are listed in Table I and labeled C in reference to Figure 1. The experiments were over a range of pressure from 0.01 torr up to 3 or 4 torr. The results of all of these experiments had a common feature in that the transition times were very short as compared to predictions from the model and also the times were only weakly dependent on pressure. An absorption trace for the transition J4 to J3 at 40 m torr is shown in Fig. 7. The fast signal formation time is typical. A second characteristic of "down" transitions, which can be seen for J4-3 in the figure, is an apparent over population of the lower level followed by a decay of the high rotational population to the Boltzmann level.

An experimental trace for the "up" transition J3-4 is also shown in Fig. 7 and obviously forms much slower than J4-3. This contrasts with the pictures generated from our rate model which predicts experimental traces for both J4-3 and J3-4 should be identical. By a simple kinetic argument it can be shown that rates for the two transitions should be equal.

To the extent that the rate constants k_{ij} from Eq. 1 are measures of the rate of population transfer from level i to level j, the measured transfer rates between $J \rightarrow J + 1$ and $J + 1 \rightarrow J$ should be equal. For short times we might write from Eq. 1:

$$\frac{dn_j}{dt} \approx k_{ij} n_{pump} \cdot \tag{7}$$

The final equilibrium value of the population in level j is (Eq. 3) $n_j \rightarrow \bar{n}_j n_{pump}$ where $\bar{n}$ is defined in Eq. 3. Scaling the transfer rate by this equilibrium population we find a rate for the transfer

$$\frac{1}{\tau_{ij}} = \frac{dn_j}{dt} / \bar{n}_j n_{pump} = k_{ij} / \bar{n}_j \cdot \tag{8}$$

But detailed balance tells us that

$$\bar{n}_j k_{ij} = \bar{n}_j k_{ji} \tag{9}$$

and so

$$\frac{1}{\tau_{ij}} = \frac{1}{\tau_{ji}} \quad . \tag{10}$$

This implies that the population (or measured absorption) as a function of time should look the same for transfer from J → J + 1 and J + 1 → J after scaling for the absolute population differences in the two final states. The simulation model verifies this as the right two pictures in Fig. 7 for transfer from J=3 to J=4 is identical to transfer from J=4 to J=3.

The experimental pictures on the left in Fig. 7 clearly show different rates for the "up" and "down" processes and in particular, it is apparent from these pictures that an additional transfer mechanism over and above rotational relaxation is preferentially transferring population in the "down" direction. It will be shown that this additional mechanism is actually lasing action between rotational levels.

A third characteristic of down rates, observed at very low pressures, was a delay between pumping the level J and the onset of population transfer to J-ΔJ. Such a delay can be seen in Fig. 8 for the J4-3 transfer at 16 m torr. Subsequent to this observation it was discovered that rotational laser action causes the rapid increase in J = 3 population. On close inspection of Fig. 8 it can be seen that the J3 population starts to increase at a very slow rate immediately after the pulse as a result of collisional transfer and this is later followed by the rapid increase.

TABLE I

Pump Laser	Probe Laser	Transition	Type of Experiment (Refer to Fig. 1)
1P4	2P2	J3-2	C
1P4	2P3	J3-3 decay	B
1P4	2P4	J3-4	A
1P5	2P2	J4-2	C
1P5	2P3	J4-3	C
1P5	2P4	J4 decay	B
1P5	2P5	J4-5	A
1P6	2P2	J5-2	C
1P6	2P3	J5-3	C
1P6	2P4	J5-4	C
1P6	2P5	J5 decay	B
1P7	2P6	J6 decay	B
1P7	2P5	J6-5	C
1P7	2P4	J6-4	C
1P7	2P3	J6-3	C
1P7	2P2	J6-2	C
1P8	2P7	J7 decay	B

Decay of Population in Rotational Level J By Collisional Transfer

Measurements were made for the rate of population decay from the level pumped by probing the level with the CW laser operating on V2-1 transitions (Experiment B, Fig. 1). Typical of absorption traces for the CW laser is the one shown in Fig. 9 for the decay of J = 5. After the initial fast pumping of the population into J = 5, there is a slower decay in the absorption trace to the new rotational equilibrium value. Assuming an overall exponential decay of the absorption, a value for τ is estimated from the curve. Data that were taken for levels J3 through J8 and over the pressure range 0.01-0.5 torr are plotted in Fig. 10 as decay rate $1/\tau$ versus pressure. A striking feature of these data is the independence of the rate on the J level pumped. One would expect the rate out of a level to be the sum of arrival rates into all other levels. Our model predicts a strong dependence on J with slower rates for high J values. The data may also be compared with independent linewidth data since the pressure dependence of linewidths is dominated by the fastest collisional process, which for HF is rotational transfer. Linewidth data (Ref. 6) have been included in Fig. 10 as the solid lines and these show the expected variation with J. The main reason for this discrepancy is that lasing between rotational levels was occurring during the measurements. This has the effect of distorting the absorption signals in not allowing them to achieve their initial pumped values and modifying the signal decay by transfer of population back from lower J levels. This is further discussed in the next section.

Peterson et al. (Ref. 7) have made measurements of rotational relaxation (decay rates) for HF by using a single laser so that the same laser transition pumped and probed the J levels. They found reasonable agreement with linewidth data. We made similar measurements by tuning both pump and probe lasers to the same v(1-0) transition (Experiment D, Fig. 1). Signals from this experiment appear as more intensely transmitted probe laser radiation due to decreasing populations in the ground state during pumping. Figure 11 shows such a signal for a CW laser on the 1P4 line probing J3 of v = 1. A comparable signal for probing J3 with the CW laser operating on the 2P3 (v2-1) line (Experiment B) is also shown. The 1P4 signal exhibits a much faster initial return to equilibrium than the one for 2P3. Data for the decay times for pumping and probing with laser lines 1P4 through 1P9 at various HF sample pressures is presented in Fig. 12. Marked on this plot, as dark crosses at 0.1 torr, are linewidth data for the lines 1P4, 1P5, 1P6 and 1P7. Reasonable agreement is found for the data from the two kinds of measurements. This leads us to conclude that Experiment D and also linewidth measurements produce rate data that are dominated by filling in of the hole created in the ground state rotational distribution rather than transfer out of the rotational level pumped. The data for transition rates $1/\tau$ from Fig. 12 are replotted as rate constants

$1/P_T$ versus the laser lines in Fig. 13. The dotted line on this plot is from our model calculations based on data from measuring rates for transitions from J up to J+ΔJ of v = 1. (It will be shown in the next section that these measurements are not materially affected by R-R lasing.) The most significant difference in the two sets of rates is that the modeled rates extrapolate to much slower values for high rotational levels. However, at the very high J level, rotational relaxation is a relatively slow process and additional contributions from velocity relaxation and vibrational relaxation are significant for the linewidth measurements.

Lasing Between Rotational Levels

In order to explain the very fast "down" rates observed in the experiments just described a process that transfers population to lower J's quickly is needed in addition to rotational relaxation. In this section we will show that rotational-rotational lasing (with wavelengths in the tens or hundreds of microns) is just such a process and we will show experimental evidence that R-R lasing is occurring in our experiment.

To see that R-R lasing is a likely explanation of the results of the transfer experiments, it is instructive to calculate the potential gain for the conditions of the experiments. From the cross section for stimulated emission σ we may calculate the gain for a given transition $J+1 \rightarrow J$ as

$$\alpha_J = \sigma_J \left\{ \left(\frac{2J+1}{2J+3} \right) n_{J+1} - n_J \right\} \tag{11}$$

where n_J is the population of the level J in molecules/cc. The cross section for stimulated emission may be written in terms of the frequency ν and Einstein coefficient A as

$$\sigma = \frac{c^2 A g(\nu)}{8\pi \nu^2} \tag{12}$$

where the lineshape function $g(\nu)$ is given by

$$g(\nu) = \frac{2(\ell n 2)^{1/2}}{\pi^{1/2} \Delta\nu_{DOPPLER}} \; e^{-4(\ell n 2)(\nu-\nu_0)^2/\Delta\nu^2_{DOPPLER}} \tag{13}$$

or at line center

$$g(\nu) = \frac{c}{\nu \sqrt{2\pi kT/m}} \tag{14}$$

Table II lists a few representative A coefficients (Ref. 8) and cross sections. It is interesting to observe that the stimulated emission cross section on these long wavelength transitions is about two orders of magnitude larger than for the corresponding V-V transition

$$\sigma_{RR}(J=1 \rightarrow 0) = 1.6 \times 10^{-13} \text{ cm}^2 \tag{15}$$

$$\sigma_{VV}(V=1 \rightarrow 0) = 1.4 \times 10^{-15} \text{ cm}^2 \tag{16}$$

With Eq.'s 11 and 12 we may estimate the gain for representative experimental conditions. We pump all of the population in the V=1 manifold into a single J level so at low pressure and before rotational transfer can move much population around

$$N_{J_{pump}} - N_{J_{pump-1}} \approx N_{J_{pump}} .$$

If we estimate an excited population of molecules of 1×10^{-4} torr (at a few tenths of a torr of total pressure) we would have for J=4→3 a gain

$$\alpha = (1 \times 10^{-4}\ \text{torr}) \left(3.5 \times 10^{16}\ \frac{\text{molecules}}{\text{cc-torr}}\right) (2.2 \times 10^{-13}\ \text{cm}^2) \qquad (17)$$

$$\approx 1\ \text{cm}^{-1}.$$

With a round trip path length of about 80 cm it is easy to expect lasing or superfluorescence in the gas cell even with essentially no mirrors. Actually the CaF_2 windows used on the gas cell are about 80 percent reflective at this wavelength and again, with the long wavelength and large gain, alignment is not critical.

To search for R-R lasing we used an experimental set-up which is diagrammed in Fig. 14. The pumping pulse from an HF laser passed through a Kel-F cell fitted with CaF_2 windows containing a sample of HF gas. The excited HF lasing on rotational transitions produced long wavelength radiation that was reflected by the CaF_2 and transmitted out of the cell through a polyethylene window. CaF_2 has reflectance of up to 90 percent over the R-R laser wavelengths (Ref. 9). A CuGe detector ($4^{\circ}K$) was used to observe the long wavelength lasing and individual laser lines were identified using a monochromator (Perkin Elmer Model E1).

Lasing at long wavelengths was observed after pumping the HF gas sample with each of 1P3 through 1P8 transitions. Table III lists the calculated (Ref. 8) and measured wavelengths. For each J level populated by the pumping, lasing was observed on transition to the next lower J level, but cascading down was not observed, possibly because such signals may be below the detection limit. In Fig. 15 traces are shown for detector observations of both the pump pulse 1P4 and the RR lasing pulse J3-2 over a range of HF pressure. Rotational lasing was seen over the range from 2 torr down to an estimated 5×10^{-4} torr (lower limit of the pressure gauge was 1×10^{-3} torr). Observation of lasing at such low pressures implies extremely high gain and these pulses at low pressure were always accompanied by a delay. This delay was found to coincide with the delayed arrival of population in the next J

level down as reported above. Lasing down to low pressure with delayed laser pulses is also evident in Fig. 16 for the transition J5-4. Table IV lists the long λ lasing tests along with pulse widths and pulse delays.

In order to estimate the gain for R-R lasing, measurements were made, pumping with 1P4 and 1P6, of the total number of molecules pumped to level J by the pump laser. This was done by measuring with a thermopyle (Eppley) the difference between incident and transmitted pumping pulse energy as a function of HF pressure. Pumping pulses are reasonably constant in energy over a period of tens of minutes, but do vary from day to day. By attenuating the pumping pulses it was possible to find the threshold value for the R-R lasing at constant HF pressure and thus estimate the optical losses for the system. Plates of combined sapphire and Irtran or germanium were used. The effects of attenuation on R-R pulse delay can be observed in Fig. 17 for J5-4 which show that increased attenuation (decreased gain) causes longer delay. The amount of delay listed in Table IV for the various tests is seen to be a function of pressure, but the values are also very dependent on the amount of energy in the pumping pulse which varies with pumping transition and to some extent with time.

The data from measurements of the energy absorbed in the cell were used to calculate the number of excited molecules (partial pressure of molecules in V=1). From our computer model of the experiment it is possible to use this information to estimate the usable gain (using Eq. 11). As soon as the pumping pulse transfers molecules from v=0 to the previously empty V=1 manifold, rotational relaxation begin to redistribute these molecules. This means that the maximum overpopulation of the pumped level is a complex function of the pulse duration and the total gas pressure. At low cell pressure a large fraction of the pumped molecules remain in the pumped J level long enough to contribute to the gain, while at high cell pressure J-1 is populated by collisional transfers almost as fast as population is pumped into J and only a small fraction of the pumped molecules contribute to the gain for the J→J-1 transition. Table V lists the excited molecular pressures, the fraction of these molecules that contribute to the gain and the maximum value of the gain (in the absence of lasing) for two different transitions at a number of pressures. At high pressures, the pumping pulse is completely absorbed in the cell and the excited molecular pressure becomes constant (independent of pressure). However, at these pressures the rotational relaxation increases with the pressure and the fraction of the excited molecules contributing to the gain goes down as does the gain itself. At low pressure, the low absorption of the pumping pulse in the cell leads to the low gain. This means that while the pressures in Table V change by over two orders of magnitude, the gain changes by only a factor of 6.

There are three measurements in Table V that were taken at constant pressure but with different attenuators in the pumping beam to reduce the pump intensity. The Germanium attenuator was sufficient to all but extinguish the lasing at this pressure-IR lasing appearing on only some pump pulses. This implies that the R-R lasing was at or near threshold for these conditions and we might take the gain at this point as an estimate of the total cavity losses at this pressure-.02 cm^{-1} (in an 80 cm round trip about 80 percent of the radiation is lost). Some of this loss comes from the loss in the "mirrors" if we call the CaF_2 flats at the ends of the cell that and some loss probably comes from absorption in the gas (or its contaminants). The losses would be expected to vary from line to line and to vary with pressure and so the entries in Table V of no lasing on 3-2 at 0.85 torr where the gain was 0.48 is not inconsistent with lasing on 5-4 at 0.05 torr and gain of 0.06.

TABLE II

J TRANSITION IN V_{21}	A (sec^{-1})	$\sigma(cm^2)$
1→0	0.02	1.6×10^{-13}
2→1	0.22	2.0×10^{-13}
3→2	0.78	2.1×10^{-13}
4→3	1.91	2.2×10^{-13}
5→4	3.79	2.3×10^{-13}
6→5	6.62	2.3×10^{-13}

TABLE III

WAVELENGTHS FOR ROTATIONAL LASING

Pump Transition	Rotational Laser Transition	Calculated Wavelength	Observed Wavelength
1P8	J7-6	36.48	36.46
1P7	J6-5	42.44	42.42
1P6	J5-4	50.82	50.78
1P5	J4-3	63.37	63.4
1P4	J3-2	84.37	84 -
1P3	J2-1	126.41	126 -
1P2	J1-0	252.59	none

Wavelengths from Meredith, Reference 8.

TABLE IV

LASING TESTS

Pump Line 1P2
Press Limit for Lasing 0.08-0.4 torr

Pressure	Pulse Width	Delay	
.35	40 ns	80 ns	

Pump Line 1P3
Press Limit for Lasing 0.03-1.9 torr

Pressure	Pulse Width	Delay	
1.3	40 ns	0	
.18	80 ns	40 ns	
.04	150 ns	400 ns	

Pump Line 1P4
Press Limit for Lasing < 0.001-2.0 torr

Pressure	Pulse Width	Delay	
1.2	50 ns	0	
.15	300 ns	40 ns	
.035	150 ns	80 ns	2 peaks at 80 ns and 150 ns delay
.015	250 ns	80 ns	2 peaks at 80 ns and 200 ns delay
.005	150 ns	500 ns	
	200 ns	700 ns	
	300 ns	1400 ns	
	500 ns	1500 ns	
	500 ns	2000 ns	

Pump Line 1P5
Press Limit for Lasing < 0.03-0.65

Pressure	Pulse Width	Delay	
.65	50 ns	80 ns	
.32	40 ns	100 ns	
.07	300 ns	100 ns	3 peaks at 100, 120, 400 ns delay
.04	150 ns	300 ns	

TABLE IV (Cont'd)

LASING TESTS

Pump Line 1P6
Press Limit for Lasing .005-2.2 torr

Press	Pulse Width	Delay	Press	P_{corr}	
2.9	20 ns	0	2.2	2.9	
2.0	20 ns	0	1.5	2.0	
1.1	100 ns	0	0.8	1.15	
.77	200 ns	0	.55	.77	two peaks at 0 and 40 ns delay
.17	250 ns	40 ns	.12	.17	two peaks at 40 and 100 ns delay
.06	250 ns	100 ns	.045	.065	two peaks at 100 and 200 ns delay
.02	200 ns	100 ns	.021	.025	two peaks at 100 and 500 ns delay
.005	100 ns	200 ns	.005	.005	two peaks at 200 and 700 ns delay

Pump Line 1P7
Press Limit for Lasing .015-7.0 torr

Press	Pulse Width	Delay	Press	P_{corr}
7.3	30 ns	--	6.6	7.3
2.5	100 ns	--	2.0	2.5
.21	400 ns	--	.15	.21
.04	100 ns	600 ns	.03	.04
.02	100 ns	1200 ns	.015	.02

Pump Line 1P8
Press Limit for Lasing .21-6.4 torr

Press	Pulse Width	Delay	Press	P_{corr}
7.2	40 ns	80 ns	6.4	7.2
3.9	200 ns	--	3.1	3.9
1.1	100 ns	80 ns	.76	1.1
.3	100 ns	300 ns	.21	.30

TABLE V

Cell Pressure (torr)	Pressure Excited Molecules (torr)	% $P_{excited}$ Leading to Gain	Gain (cm^{-1})	Delay (ns)
J5→4				
3.5	2.9×10^{-4}	5	.11	(no lasing)
.85	2.9×10^{-4}	17	.38	40
.3	2.7×10^{-4}	32	.66	40
.17	1.6×10^{-4}	41	.49	70
.05	5.2×10^{-5}	61	.24	120
.03	2.2×10^{-5}	67	.11	160
.05[1]	2.2×10^{-5}	61	.10	130
.05[2]	1.3×10^{-5}	61	.06	200
.05[3]	3.9×10^{-6}	61	.02	220
J3→2				
.85	4.4×10^{-4}	15	.48	(no lasing)
.3	4.4×10^{-4}	28	.91	
.17	4.4×10^{-4}	36	1.15	35
.05	2.7×10^{-4}	53	1.05	60
.03	2.2×10^{-4}	57	.93	80
.017	9.9×10^{-5}	62	.45	120
.007	7.1×10^{-5}	67	.35	160

(1) No Attenuator
(2) Sapphire and Irtran Attenuator in Pump Beam
(3) Germanium Attenuator in Pump Beam

Population Transfer - Combined Lasing and Rotational Relaxation

A simple model of the rotational-rotational lasing process was added to the rotational relaxation model to improve the computer simulation of the experiments. In this model the photon flux, through stimulated emission, adds two terms to the population transfer rate equation (Eq. 1).

$$\frac{dn_J}{dt} = (n_{J+1} - n_J)\ \sigma_J\ I_J - (n_J - n_{J-1})\ \sigma_{J-1}\ I_{J-1} + \text{rotational collisional relaxation terms.} \tag{18}$$

Here I_J is the photon flux in photons/cm^2-sec from the transition J+1 → J. Population changes due to spontaneous emission are small and have been neglected. This population rate equation is now coupled by the photon flux, I, to a rate equation for the photon field (in a closed cavity) written as

$$\frac{dI_J}{dt} = I_J C(\alpha_J - \gamma_J) + n_{J+1}\ C\ \Omega\ A_J \tag{19}$$

where γ_J are the total losses for J+1 → J treated as distributed uniformly throughout the medium and Ω is the solid angle of the beam from one end of the cavity. The first term will produce a net exponential gain in the photon flux of $(\alpha - \gamma)$ while the second term represents spontaneous emission. The fluorescence term is necessary here to correctly describe the time it takes for the rotational-rotational lasing to begin. At the low pressure at which some experiments were conducted and with the long spontaneous lifetime for these lines ($1/A \sim 1$ sec), it takes a quite measurable time to get even one photon from spontaneous emission into the solid angle, Ω, of the beam. In fact, we can anticipate a delay time of the order of

$$\tau_{DELAY} \geq \frac{1}{n\Omega VA} \tag{20}$$

to get just one photon into Ω in the volume V near one end to begin the lasing. With the very high total gain, αL, one photon quickly builds the photon flux through 10-12 orders of magnitude even with the high cavity losses. (Estimates show that even at these long IR wavelengths, the thermal black body photon density at 300°K is negligible.)

The total time delay between the onset of the pumping pulse and the onset of the IR lasing has a number of contributions including the delay time just calculated. The rise time of the pumping pulse and the net gain (α-γ) also contribute to the total delay time.

To demonstrate the effect of the R-R lasing on the population transfer process, calculations were run with the augmented computer model and the constants from the previous "up" transfer experiments (Eq. 6). In a case where J=5 is pumped and at a total pressure high enough to make τ_{DELAY} small, Fig. 18 shows the comparison of the population as a function of time for R-R lasing compared to the no-lasing case where γ (losses) is set to infinity. Figure 18b shows the population in J=5, the level being pumped. When R-R lasing occurs, some population is quickly transferred to the next lower level (J=4) and the net population reaching J=5 is reduced.

As discussed above, in the absence of lasing, the net rate out of the pumped level is related to linewidth measurements. Here, however, a large population is being pumped from J to J-1 by a fast, noncollisional process and the net loss rate after the lasing stops is reduced below the value predicted from linewidths.

Figure 18a clearly shows the population being rapidly transferred to J=4 by the R-R lasing. In fact, the level is overpopulated relative to the final Boltzmann equilibrium and the characteristic shape seen in the down transfer experiments is produced.

Figure 18c shows the population evolution in J=6. Here the R-R lasing makes the smallest difference. Since some population is removed from J=5 before it can be rotationally transferred to J=6 the rate into J=6 is reduced slightly. However, the change is small, and this leads us to believe that the rates predicted by the model (Eq. 2) and the constants (Eq. 6) derived from the "up" transfer experiments done earlier are substantially correct.

At low pressure, these model calculations show the correct delay behavior of the R-R lasing pulse but the deficiencies of the model now become evident in the population time evolution and in the duration of the R-R lasing. Figure 19a shows examples of the computer simulation at 0.036 torr when J=5 is pumped. We see a delay of about 110 ns when the experimental measurement was 120 ns (Table III). The losses here have been reduced to an artificially low level (.003/cm) to lengthen the pulse to about 40 ns duration. The IR lasing commences very suddenly, distorting the population (Fig. 19b). It is believed that a model that treats the cavity as a one pass laser rather than distributing the total losses throughout the cavity would give significantly improved population evolution results. However, this model is sufficient to demonstrate the correctness of the physical picture underlying the calculation.

To illustrate the behavior of the R-R lasing pulse delay and the effect on the population transfers, Fig. 20 shows results for a range of pressures when J=5 is pumped and J=3, 4, 5 and 6 probed. The first column exhibits the pumping pulse (below) and the subsequent long wavelength IR pulse (above). The delay is clearly shown to be pressure dependent, varying from near zero at 0.85 torr to 140 ns at 0.027 torr. Also note that a 3.5 torr no long wavelength IR appears. At this high pressure rotational relaxation proceeds so quickly that J=4 fills almost at the same time as J=5 and only 6 percent of the pumped population appears as a net population difference between 5 and 4 at any time. The gain α_J, for this case, is actually less than the value achieved at 0.027 torr. Since pressure dependent absorption losses in the gas are larger by more than a factor of 100 it is hardly surprising that there is no net gain. In this case what gain exists would be distributed in a very nonuniform manner in the gas cell due to the exponential absorption.

The column labeled 5-5 of Fig. 20 shows the absorption from the population pumped into the J=5 level along with the long IR radiation (above). At the lowest pressure, population begins arriving in the level J=5. After 140 ns, the long wavelength radiation appears and the population increase levels off abruptly as population is rapidly transferred to J=4. After the R-R lasing turns off, the collisional rotational relaxation tail appears. At higher pressures, the delay is shorter and the effect on the population occurs earlier in the pumping part of the cycle.

The column 5-4 exhibits the 5→4 "down" transfers. At low pressures, the transfer commences with the R-R lasing and is very rapid while the R-R laser is running. At progressively higher pressures, little change in the basic transfer rate is observed in that the rate depends more on the IR lasing (with little direct dependence on pressure) rather than rotational transfer (which varies directly with pressure). Also at higher pressures smaller population excesses occur.

The column 5-3 shows the transfer 5→3 and 5→4→3. At the lowest pressure the transfer begins after laser transfer from 5→4 well after the onset of IR lasing. At the next two higher pressures (.15 and .3 torr) a delay occurs between the IR lasing pulse and the onset of transfer into J=3. Here however, the transfer rate is very fast with sharp edges implying 4→3 cascade lasing although direct evidence of this transition was not found. At .85 torr the delay has disappeared and rotational collisional transfer is proceeding rapidly enough to inhibit the lasing on the cascade 4→3 transition. The transfer rate is observed to be <u>slower</u> than the rate at the lower pressures as this transfer now occurs solely through collisional transfer. We believe these four pictures constitute strong presumptive evidence for cascade lasing after the 5→4 lasing occurs.

The column 5-6 contains the 5→6 "up" transfers. This data is little affected by the long wavelength transfer and the transfer rates are seen to be smooth and increase directly with the pressure.

The computer simulation model was also used to estimate the importance of R-R lasing for large scale chemical lasers. Using parameters appropriate to a 2-10 kW HF chemical laser, and a distribution of rotational population from the chemical reaction as given by Polanyi (Ref. 10) (peaked between J=7-8 for HF) the model shows significant R-R lasing flattening the rotational distribution quickly and producing a few hundred watts of long wavelength IR radiation.

Vibrational-Rotational Transfer

It is now accepted on the basis of theoretical arguments initiated by Shin (Ref. 11) that the fast rate for vibrational relaxation of HF is due to vibration-rotation transfer rather than vibration-translation transfer. Thus molecules in V = 1 (or other vibrational levels) can transfer to V = 0 at high rotational levels through nearly resonant energy exchange. There has until now been no direct experimental evidence for this pathway. We have used the double resonance method in an attempt to gain such evidence. Because of several difficulties the attempt was only partially successful.

The experiment used a 1P4 pump laser line to populate J3 of V = 1 and a probe operating on lines 1P7 up to 1P10 to detect population arrival up to J = 10 of V = 0. This experiment is denoted as E in Fig. 1. The laser could not be made to operate on transitions higher than 1P10, whereas one would like to use lines up to 1P13. The 1P10 line itself had but marginal strength and stability. The CW probe radiation was chopped for a separate measurement of the intensity I_o to be ratioed with the intensity I of the absorption signal after the pulse for determining the absolute population transferred to each probed J level.

The probe laser intensity change is shown in Fig. 21 - probing J8 of V = 0 after pumping J3 of V = 1. From the trace it can be seen that population does indeed arrive in this high J level and the rate of arrival of about 4×10^4 sec^{-1} $torr^{-1}$ is approximately the vibrational relaxation rate (6×10^4 sec^{-1} $torr^{-1}$). The apparent gain near the front of the trace is typical and causes a distortion of the curve and error in determining the rate. The increased transmission is due to reshuffling of the rotational distribution in V = 0 after the pumping depletes one level. Data taken for the various lines and over a range of pressure consistently gave rates close to the vibrational relaxation rate. The intensity measurements gave a result that about 0.02 torr (at 1 torr total HF pressure) was in each of J7, 8, 9 and 10 at the peak of the signal trace. We conclude that this lack of definition of the rotational distribution during transfer results from insufficient sensitivity of the measurements. In general, however, the signals were consistent with vibrational relaxation times.

Velocity Redistribution

Since the pump laser pumps HF molecules to V, J at line center (to within ± 25 MHz), these molecules reside within a narrow velocity range at the center of the Doppler profile. It was possible to tune the CW probe laser to frequencies displaced from line center and observe the transfer rate of molecules into other velocity classes. Figure 22 shows the Doppler line shape traced by tuning the optical cavity of the CW laser. Two tuning positions are shown: A at line center and B displaced from line center by 120 MHz. The absorption traces for these positions are labeled A and B. At position A the pumping and rotational decay of the population follows the usual course. At B, the rotational processes are completed by the time the molecules have spread out in velocity to the 120 MHz position. Data for this kind of measurement was obtained at 37 m torr, 50 m torr and 122 m torr with scope pictures at several tuning positions.

Using the data in Fig. 22 we find that at $v = 0$, rotational relaxation and R-R lasing causes the population to decay in about 1μs. The second trace, B, taken at 120 MHz also has a time constant of about 1μs. Taking into account the fact that the process of transfer of population out of the level affects the apparent rate of collisional rearrangement we find an effective rate of velocity relaxation of 3.8μs at .037 torr or a rate of 7.1×10^6/sec-torr at 120 MHz (2.6×10^4 m/sec). For this level (J = 3) the total rotational loss rate is 1.3×10^8/sec-torr. For HF, the hard sphere scattering rate at 300°K ($k \sim v\sigma$) would be about 1×10^6/sec-torr. Therefore, velocity relaxation is about an order of magnitude faster than gas kinetic but still an order of magnitude slower than rotational relaxation.

REFERENCES

1. Hall, R. J.: IEEE J. Quant. Elec. 12, 453 (1976).

2. Hinchen, J. J. and R. H. Hobbs: J. Chem. Phys. 65, 2732 (1976).

3. Deutsch, T. F.: Appl. Phys. Lett. 11, 18 (1967).

4. Skribanowitz et al.: Appl. Phys. Lett. 20, 428 (1972).

5. Goldbar, J., R. M. Osgood and A. Javan: Appl. Phys. Lett. 18, 167 (1971) Also L. M. Peterson et al. have measured HF pulsed laser linewidths to be only 3 MHz wide.

6. Lovell, R. J. and W. F. Herget: J. Opt. Soc. Am. 52, 1374 (1962) and W. F. Herget, W. E. Deeds, N. M. Gailar, R. J. Lovell, and A. H. Nielsen, J. Opt. Soc. Am. 52, 1113 (1962).

7. Peterson, L. M., G. H. Lindquist and C. B. Arnold: J. Chem. Phys. 61, 3480 (1974).

8. Meredith, R. E. and F. G. Smith: Willow Run Laboratories, The University of Michigan, Report No. 84130-39-T(II), 1971 (unpublished).

9. Strong, J.: Concepts of Classical Optics, W. H. Freeman and Co., 1958, p. 592.

10. Polanyi, J. C. and K. B. Woodall: J. Chem. Phys. 57, 1574 (1972).

11. Shin, H. K.: Chem. Phys. Lett. 10, 81 (1971).

LIST OF PUBLICATIONS

Planned publications by Authors J. J. Hinchen and R. H. Hobbs:

1. Rotational population transfer in HF
2. Lasing on rotational transition of HF
3. Combined lasing and collisional processes in HF population transfer
4. Evidence for vibration-rotation population transfer in HF

Presentation:

"Rotational Relaxation in HF" by J. J. Hinchen and R. H. Hobbs at Air Force (OSR) Contractor's Meeting, Albuquerque, New Mexico, May 16-17, 1977.

FIG. 1

ENERGY LEVEL DIAGRAM FOR HF

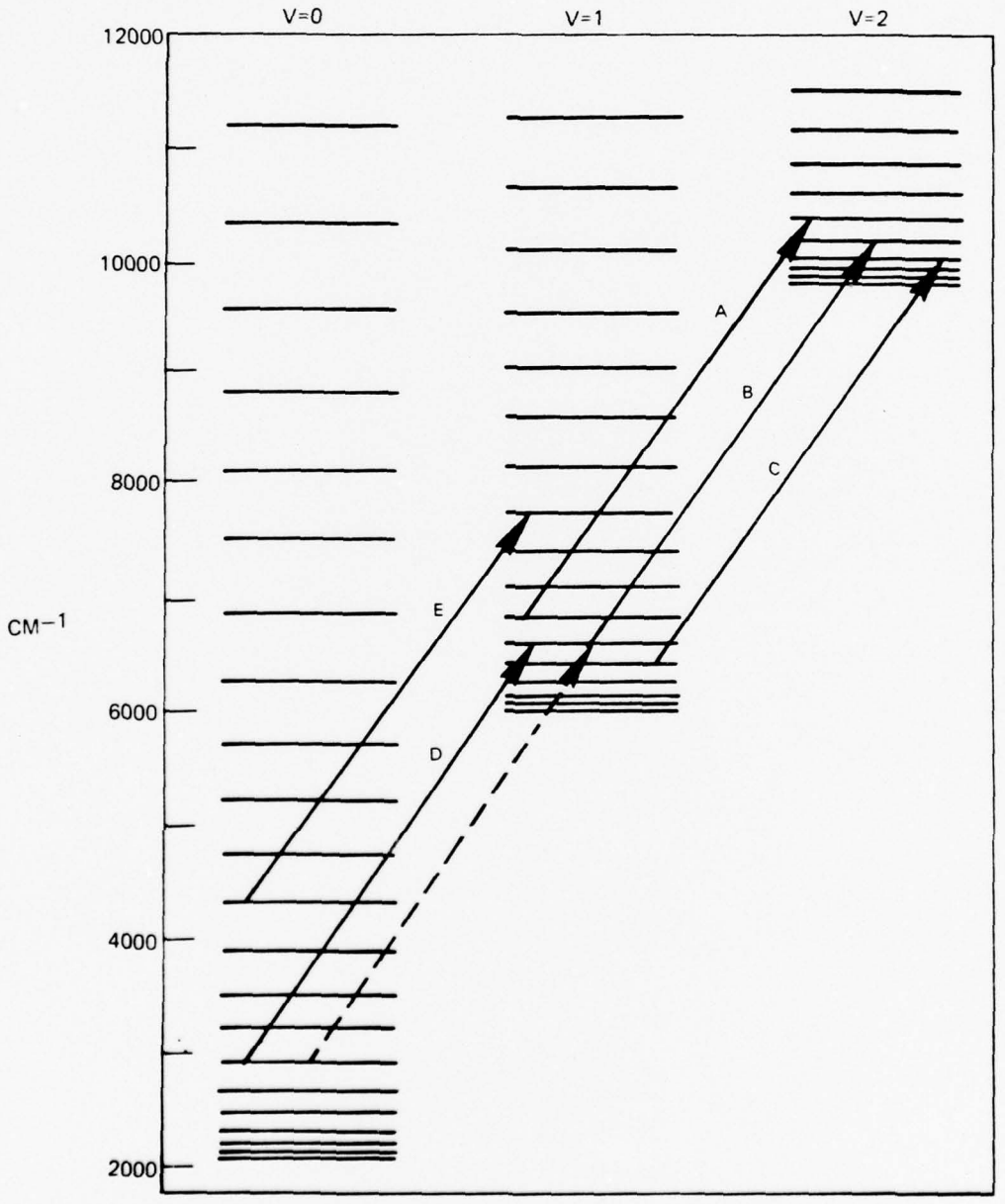

77-08-206-11

FIG. 2

COMPARISON OF MODEL AND EXPERIMENT

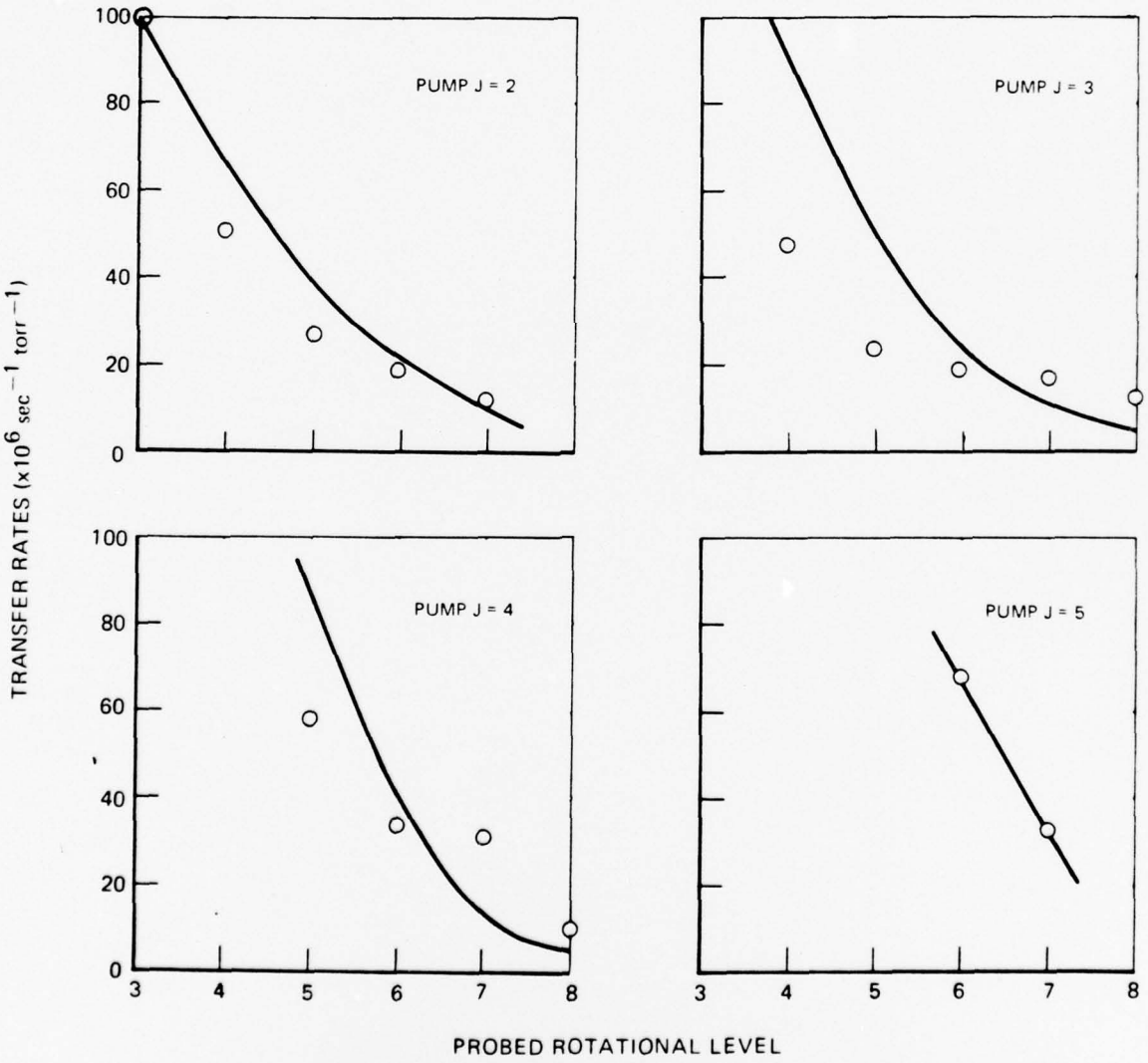

R06–171–31

PUMP LASER PULSE 1P4

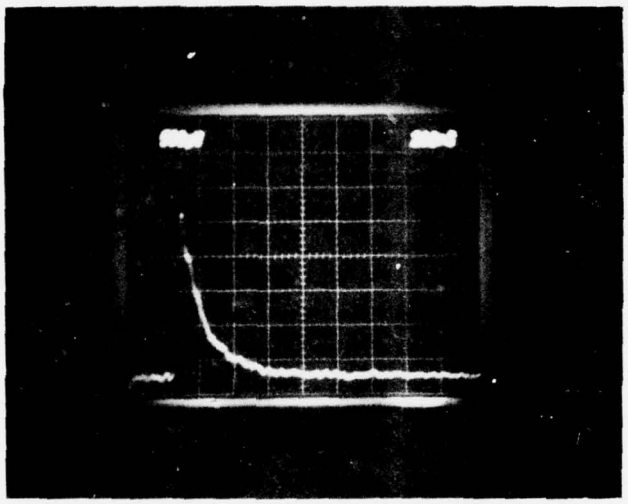

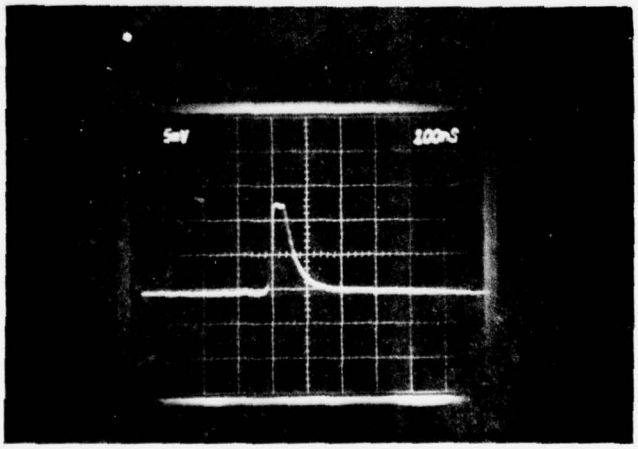

Q-SWITCHED PULSE

FIG. 4

FREQUENCY SCAN OF PUMPING PULSE

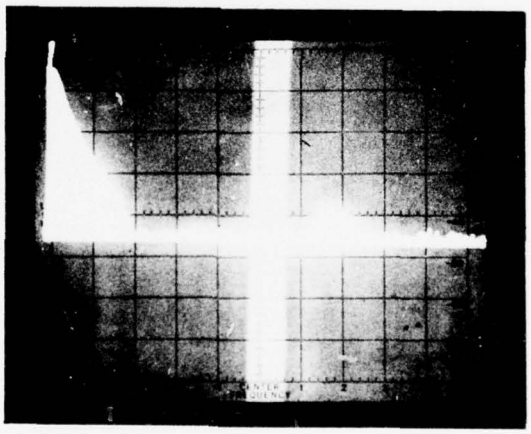

10 MHz/DIV.

FIG. 5

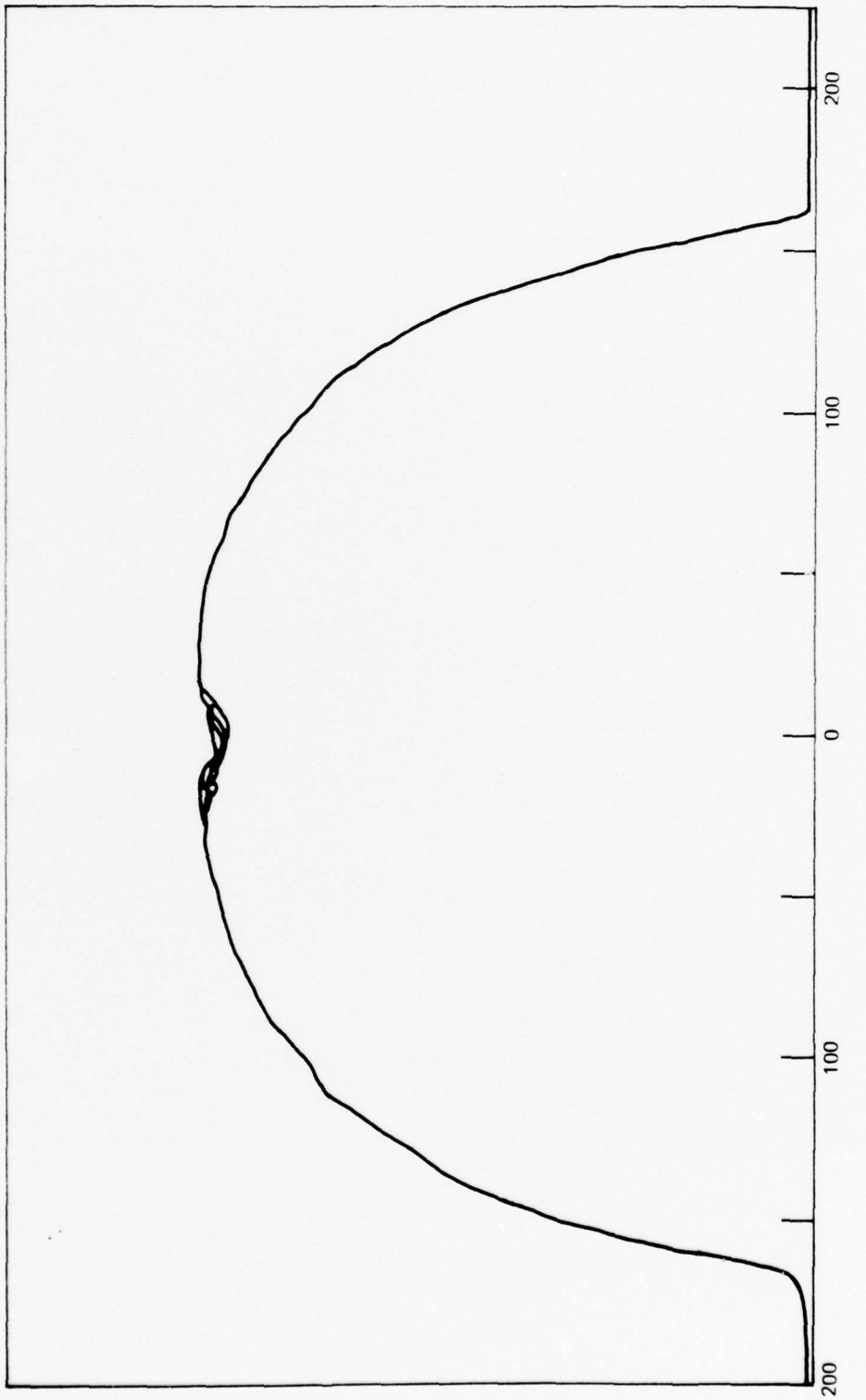
LASER INTENSITY VS FREQUENCY
LASER LINE $P_{2-1}(5)$
LASER INTENSITY
200
100
0
100
200
FREQUENCY (MEGAHERTZ)

FIG. 6

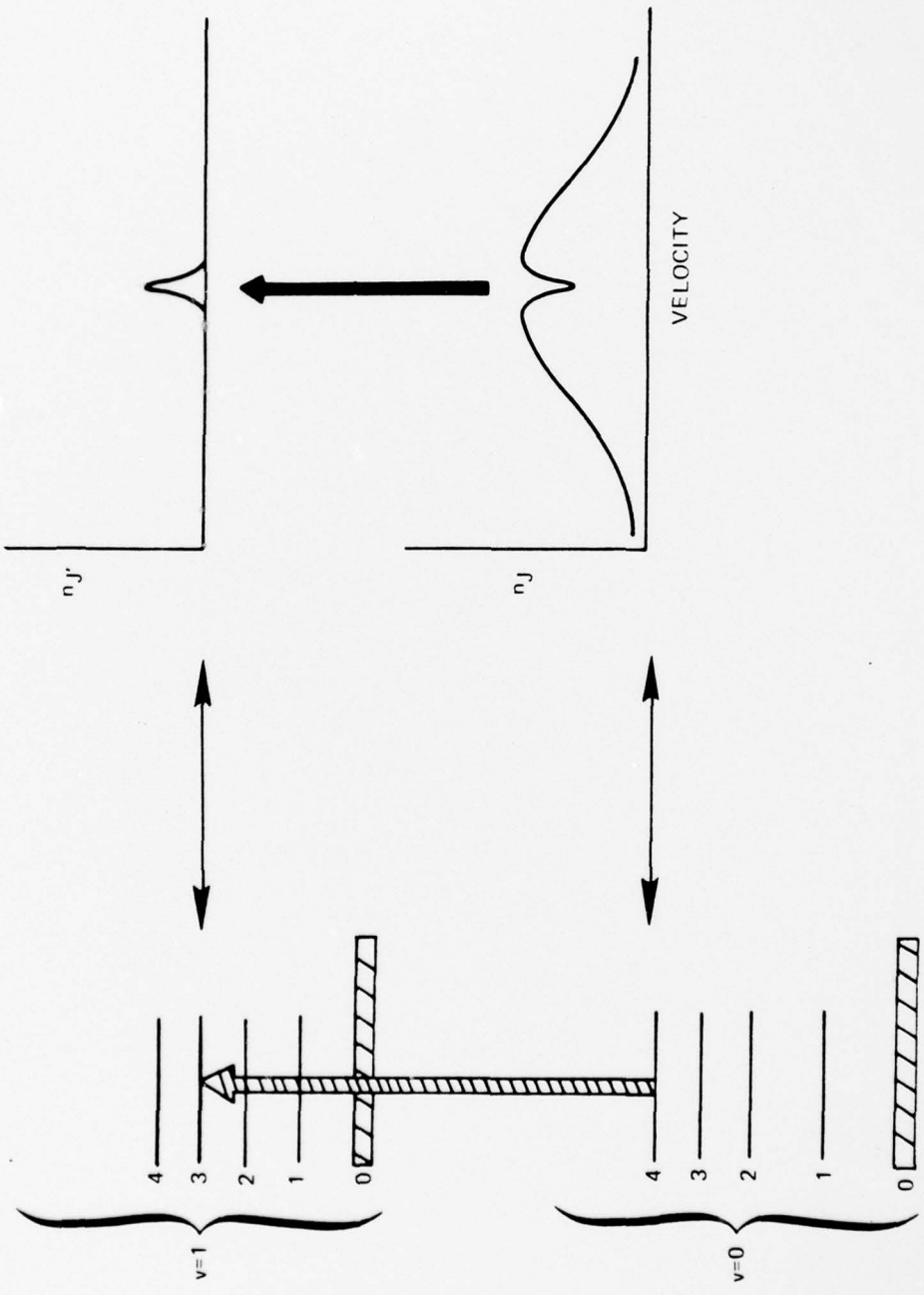

77-08-206-12

FIG. 7

HF TRANSITION TIMES

(40m TORR)

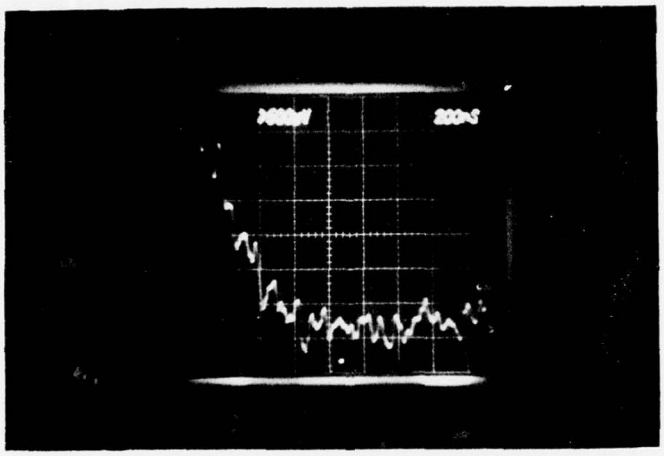

J3-4

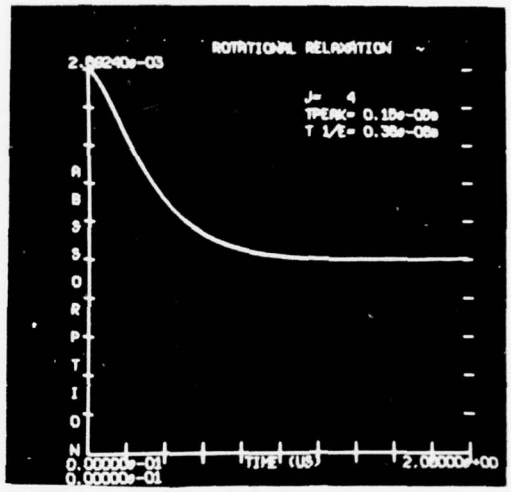

J3-4

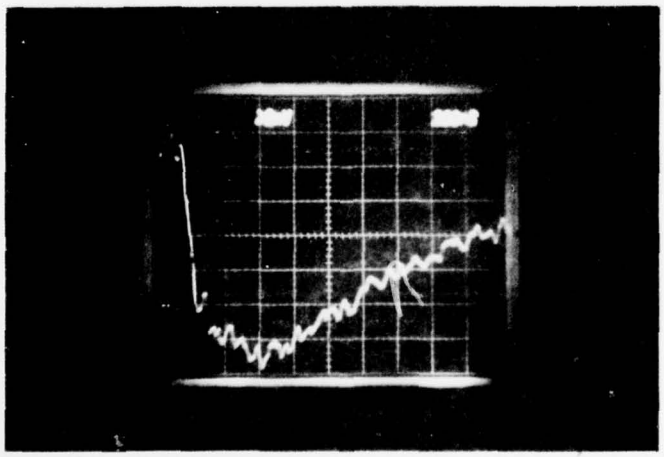

J4-3

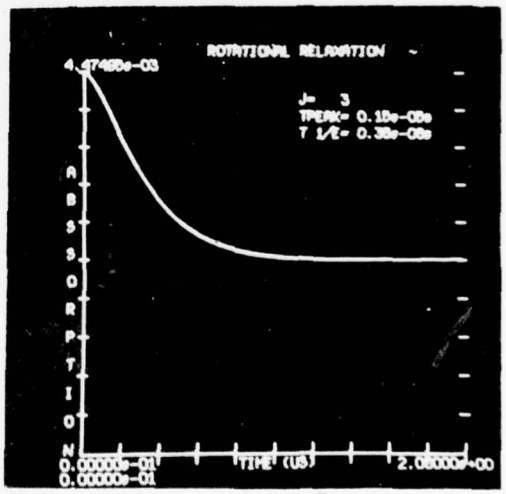

J4-3

POPULATION TRANSFER J4-3

PRESSURE 0.016 TORR

TOP TRACE - 1P5 PUMPING PULSE

BOTTOM TRACE - 2P3 PROBE

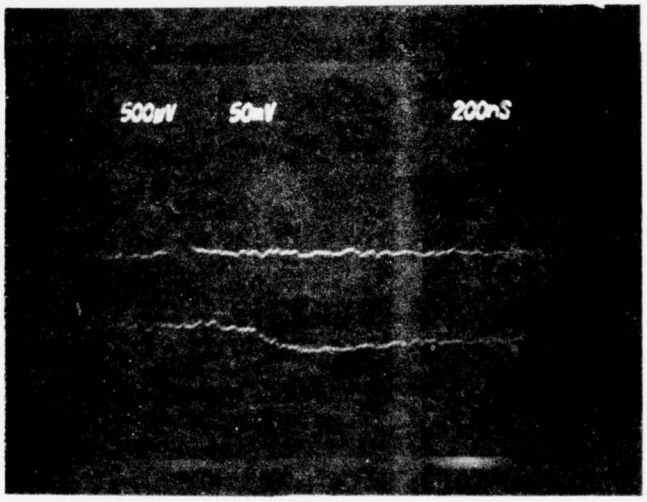

PROBE SIGNALS

PUMP AND PROBE J5

TOP TRACE – Q-SWITCHED PUMP PULSE

PRESSURE – 0.13 TORR

NOTE: SIGNAL RETURNS TO NEW EQUILIBRIUM LEVEL

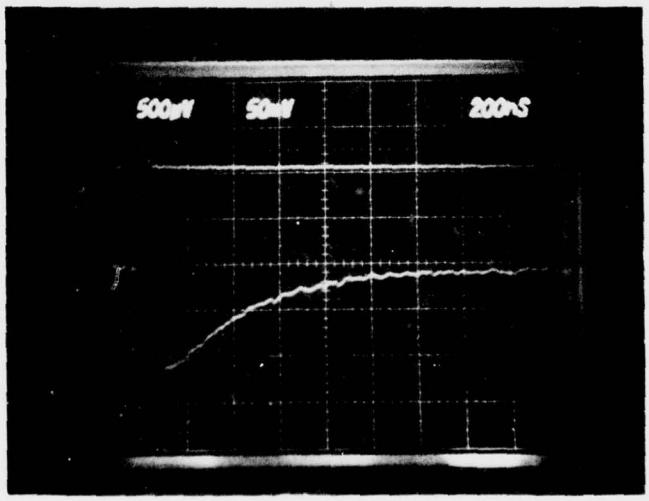

RELAXATION TIMES–PROBE V = 1, J

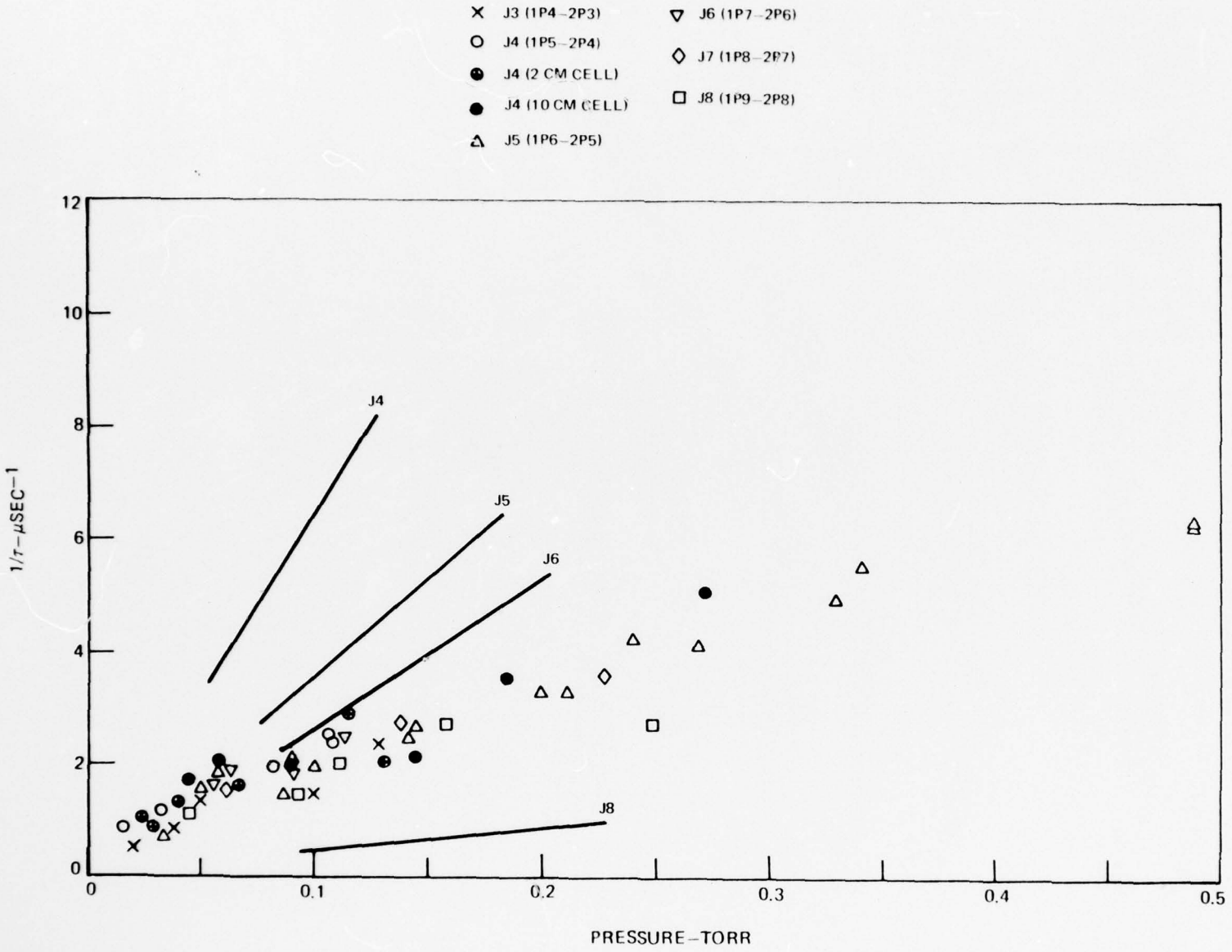

R77–952595–1

77–08–206–9

FIG. 10

PROBE SIGNALS–PUMPING 1P4

(11m TORR)

PROBE 2P3

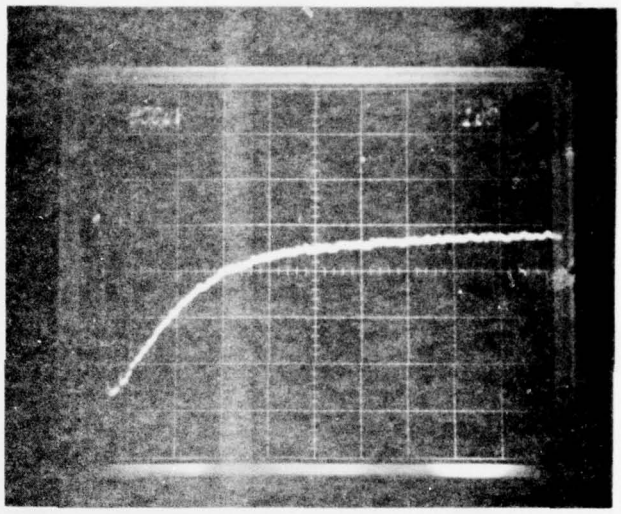

PROBE 1P4

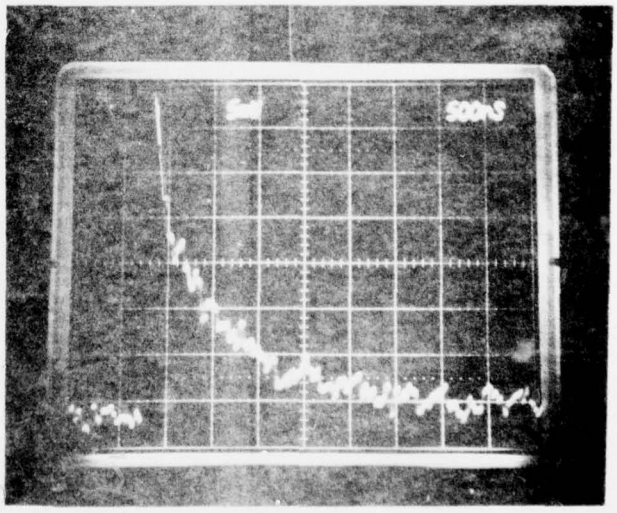

FIG. 12

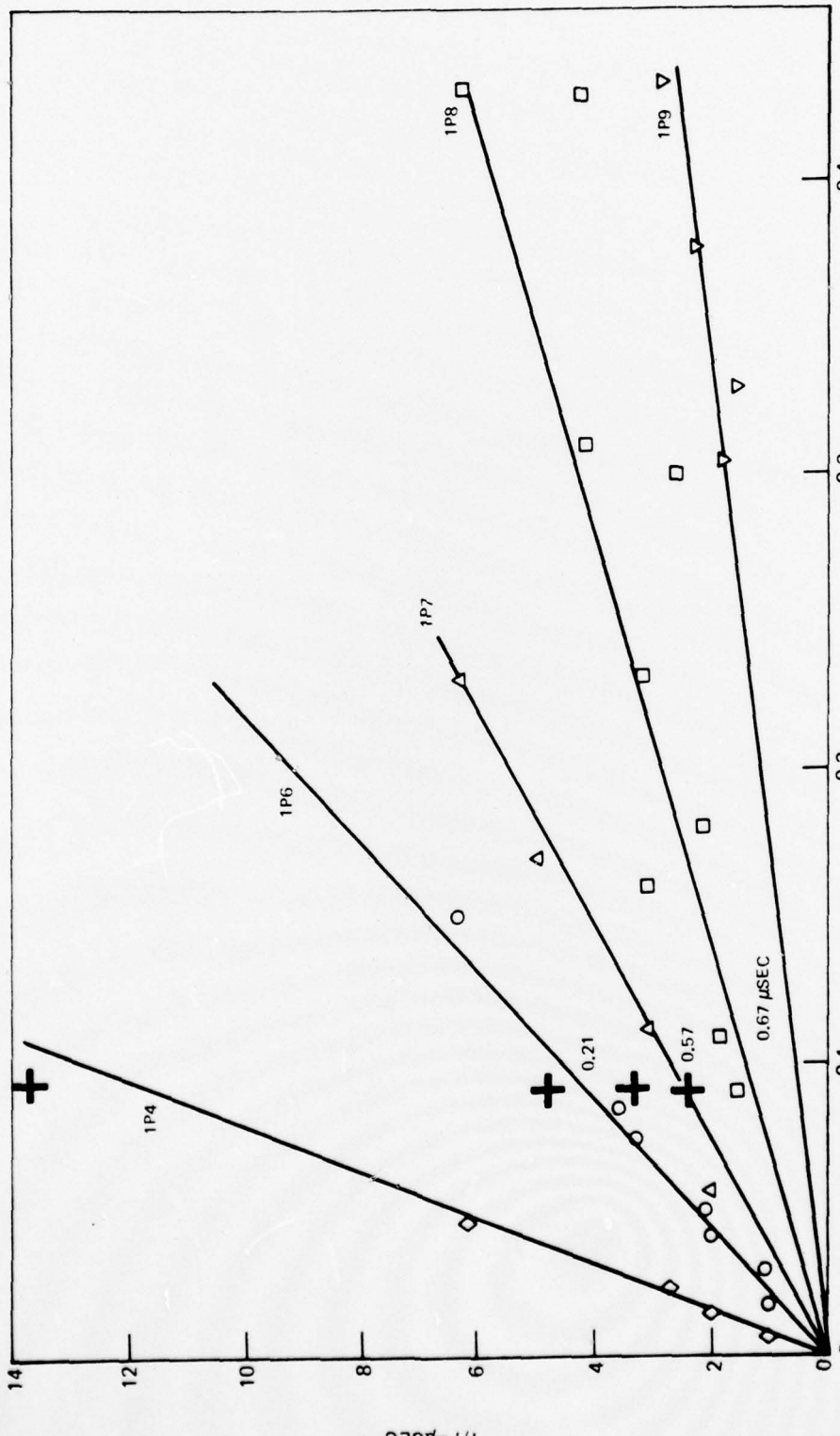

77–08–206–10

FIG. 13

RELAXATION RATES–PROBE V(1–0)

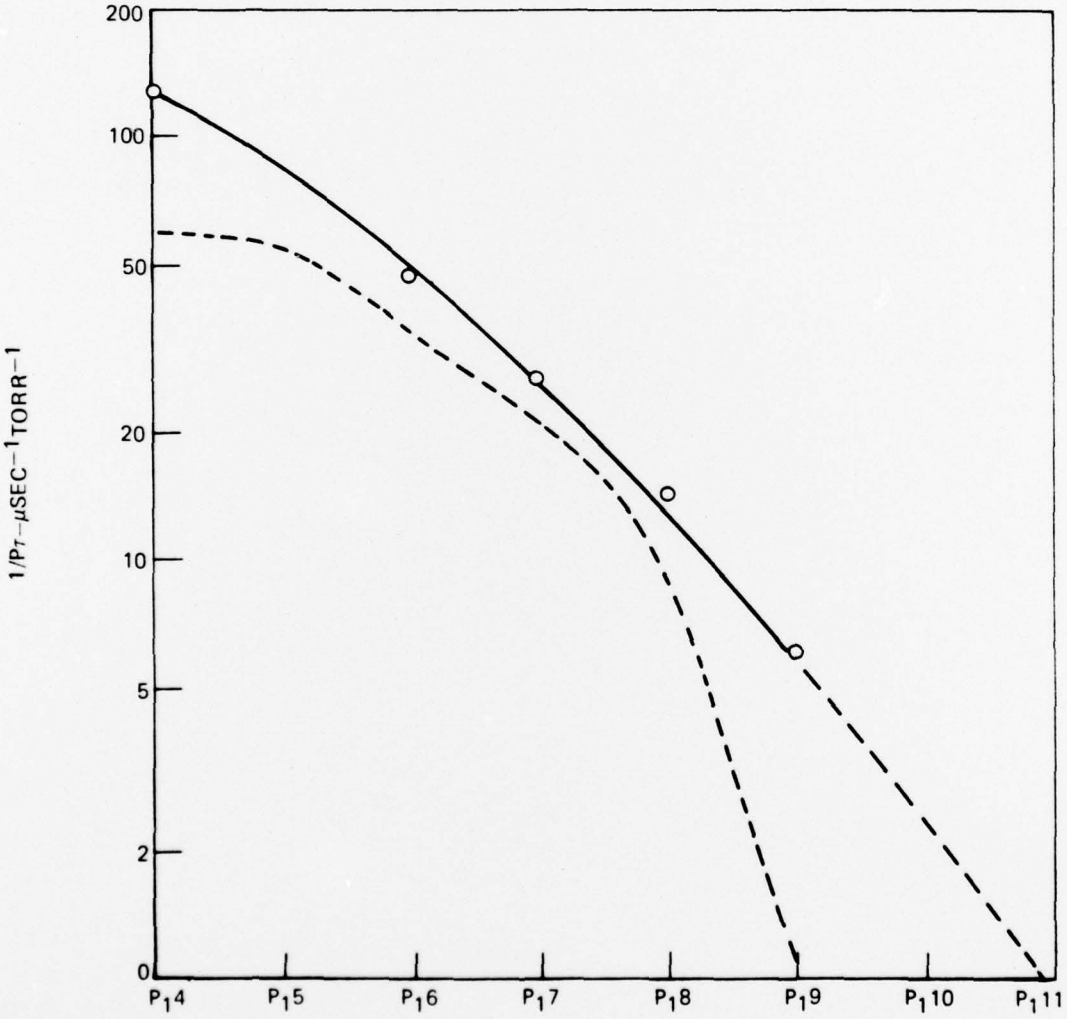

77–08–206–13

FIG. 14

APPARATUS FOR ROTATIONAL LASING

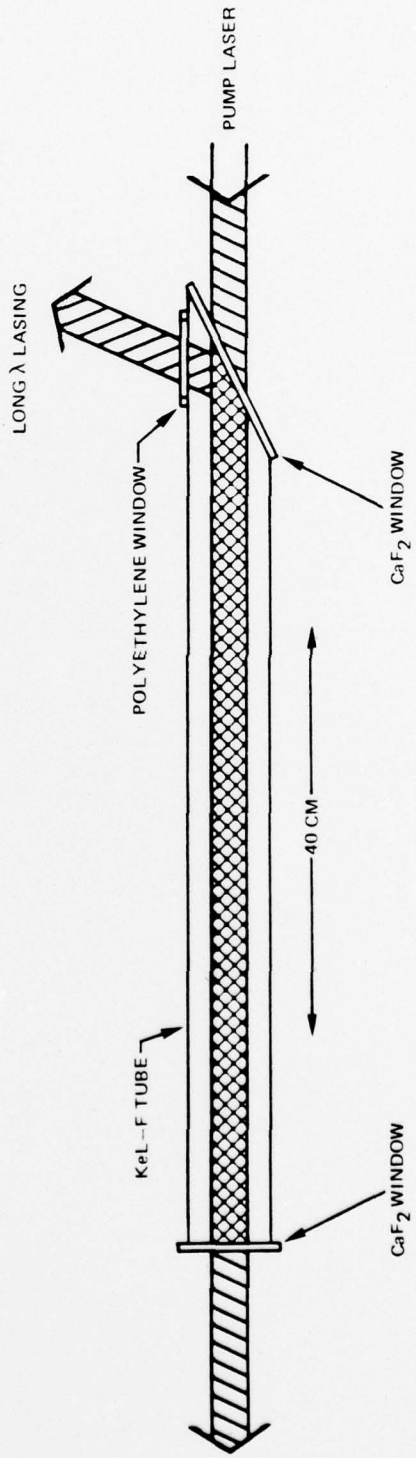

FIG. 15

R-R LASING J3-2 AT VARIOUS PRESSURES

(BOTTOM TRACE-R-R, TOP TRACE-1P4 PUMPING PULSE)

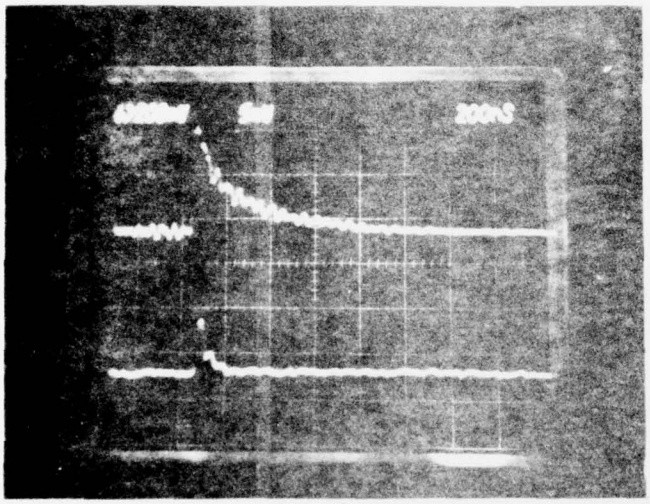

1.0 TORR

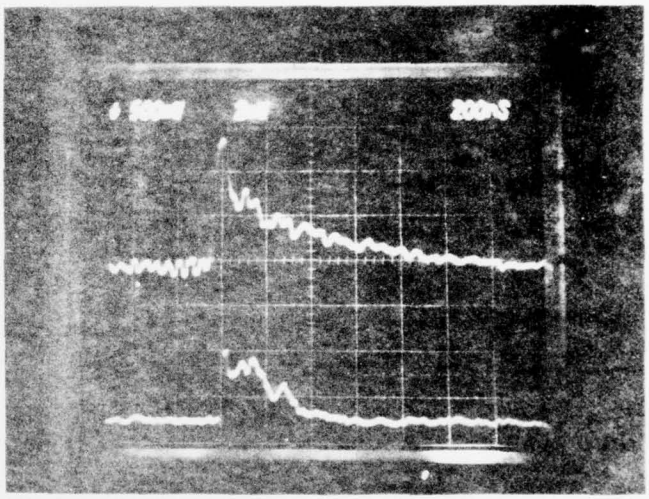

0.15 TORR

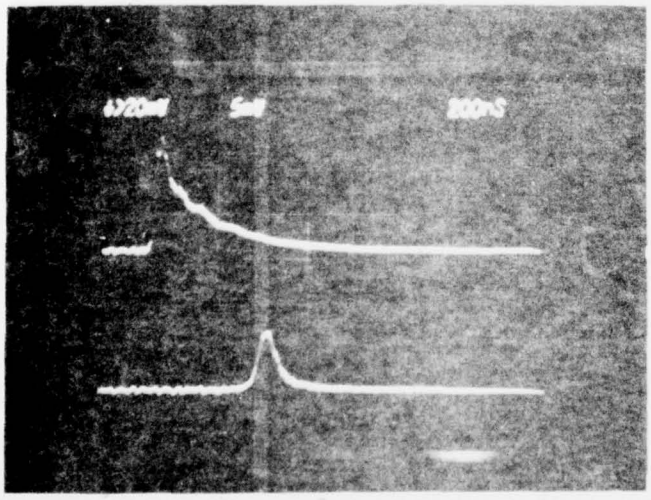

1×10^{-3} TORR

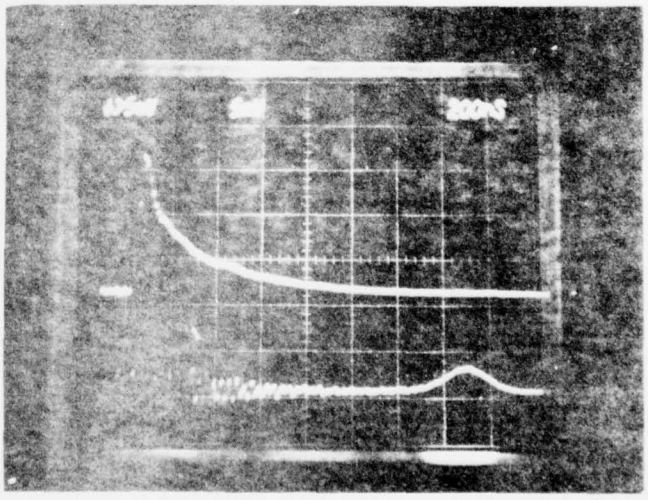

ABOUT 4×10^{-4} TORR

R–R LASING J5–4 AT VARIOUS PRESSURES

(TOP TRACE – R–R, BOTTOM TRACE–1P6 PUMPING PULSE)

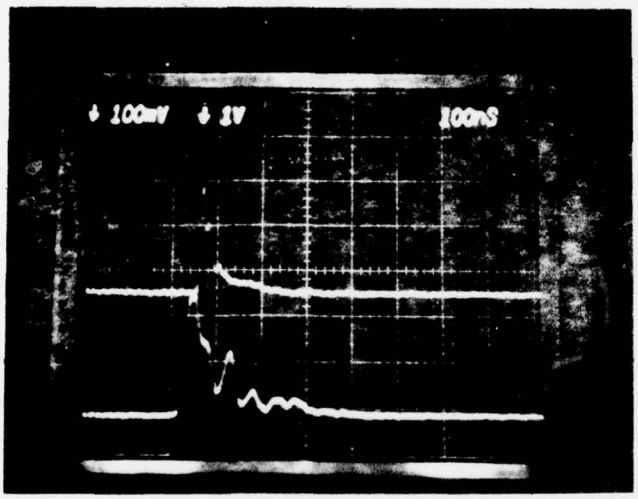

0.85 TORR

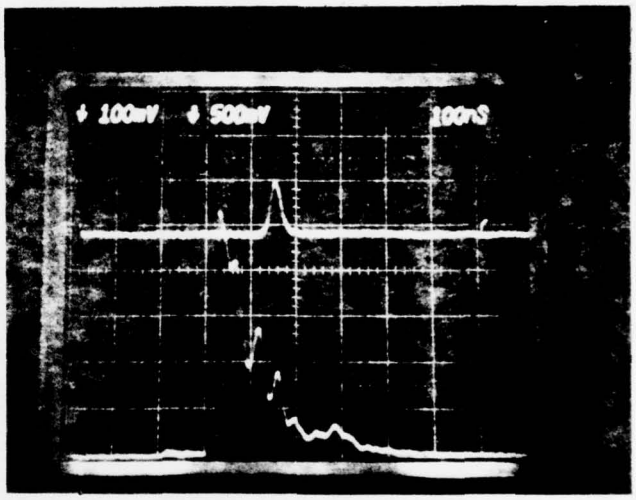

0.05 TORR

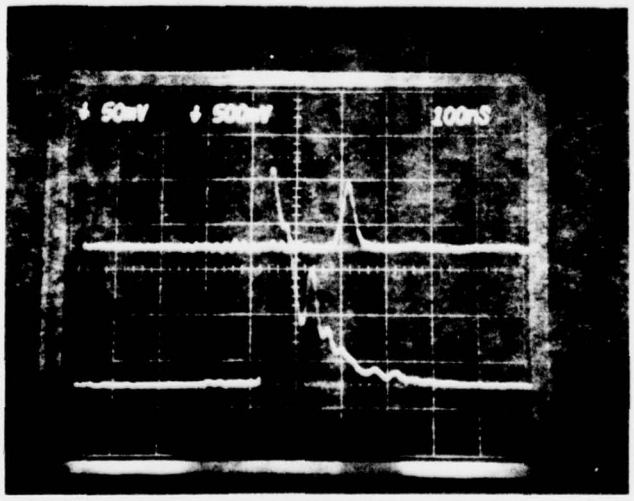

0.03 TORR

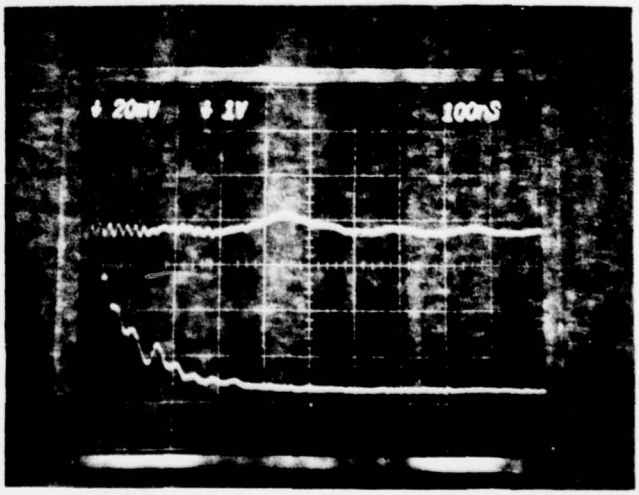

0.017 TORR

R77–952595–1

FIG. 17

R–R LASING J5–4 WITH VARIOUS ATTENUATION AT 0.05 TORR

(TOP TRACE – R–R, BOTTOM TRACE –1P6 PUMPING PULSE)

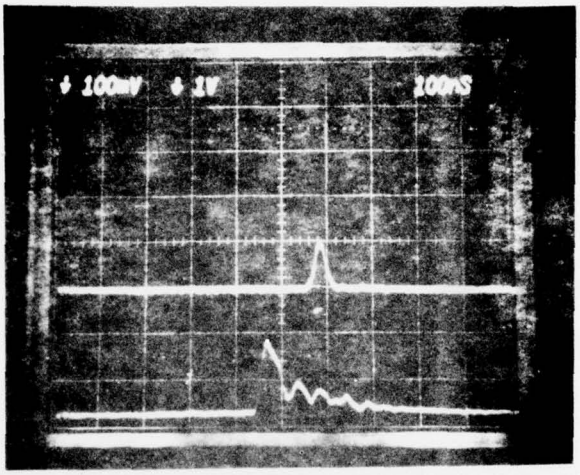

NO ATTENUATION

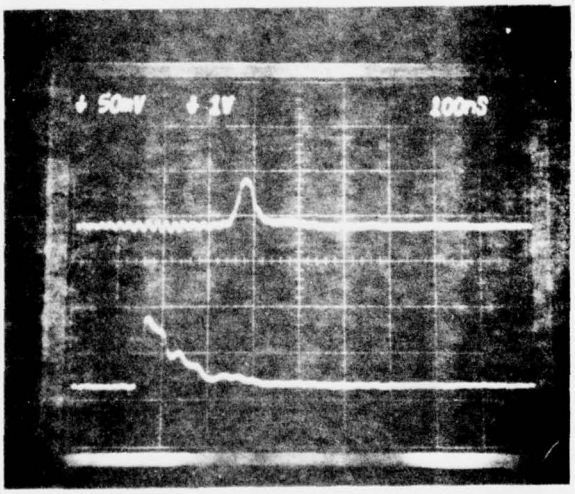

40% ATTENUATION

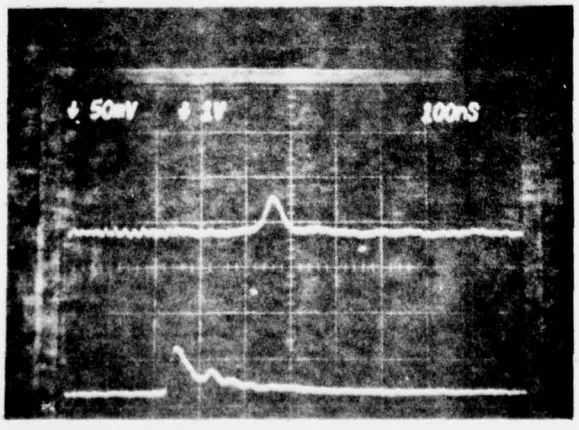

82% ATTENUATION

FIG. 18

COMPUTER MODEL OF R–R LASING AND NON–LASING BEHAVIOR

PRESSURE 0.1 TORR

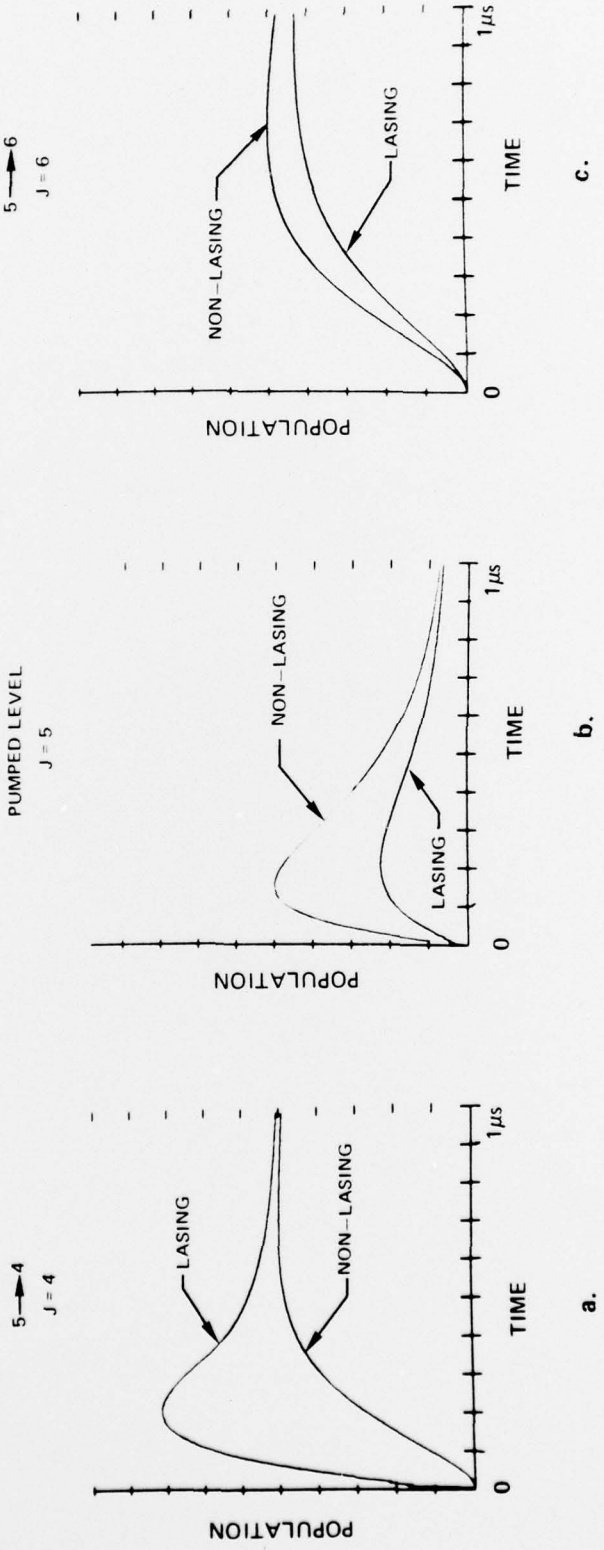

FIG. 19

COMPUTER MODEL OF R-R LASING AT LOW PRESSURE

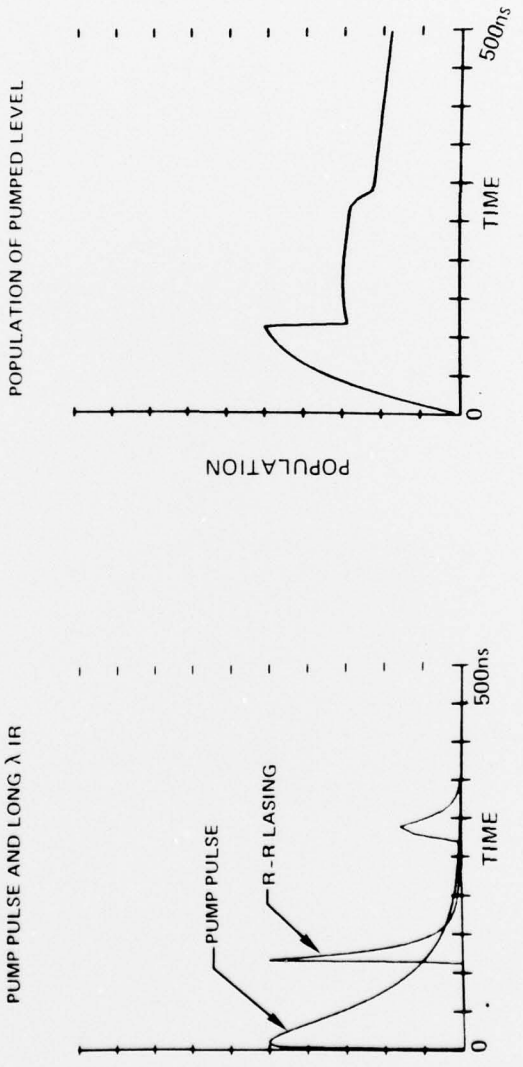

R-R LASING AND POPULATION T

TOP TRACE – R-R

BOTTOM TRACE –

TOP TRACE – R-R LASING
BOTTOM TRACE – PROBE BEAM

3.5 TORR

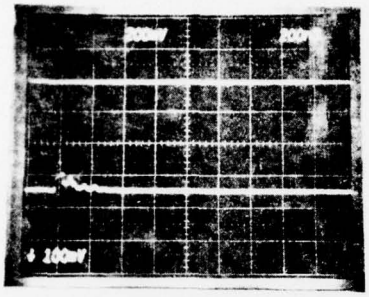

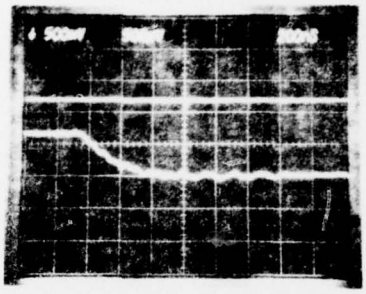

0.85 TORR

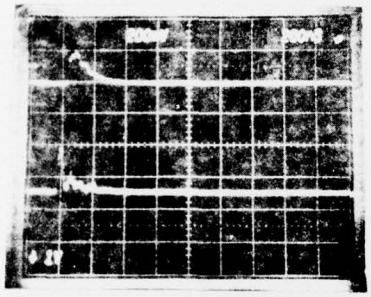

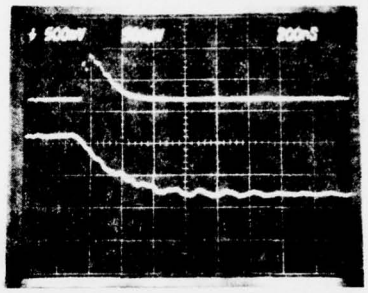

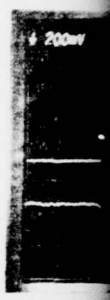

0.30 Torr

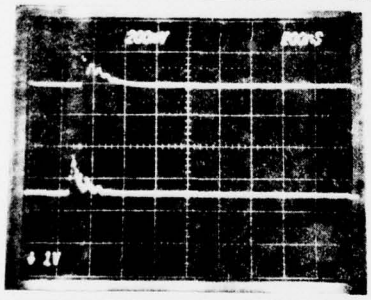

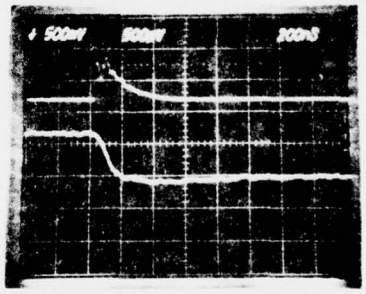

0.15 TORR

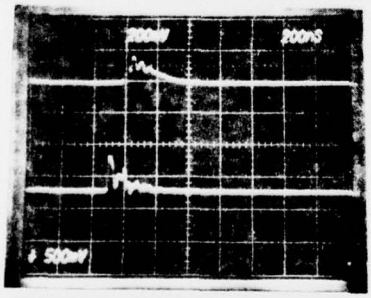

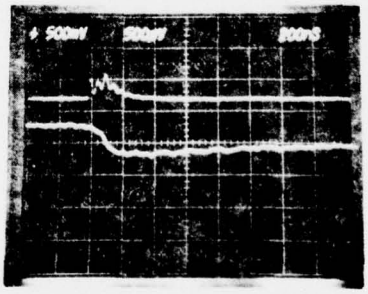

0.027 TORR

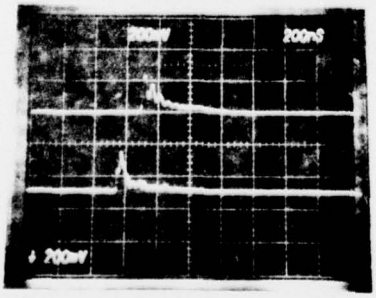

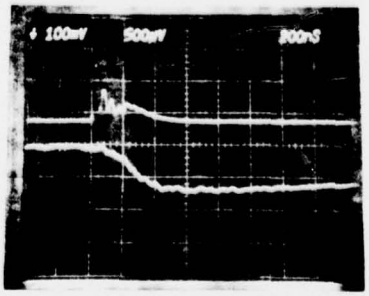

2

FIG. 20

ULATION TRANSFER TIMES FROM J TO J'
ACE – R–R LASING
M TRACE – PROBE BEAM

5–4

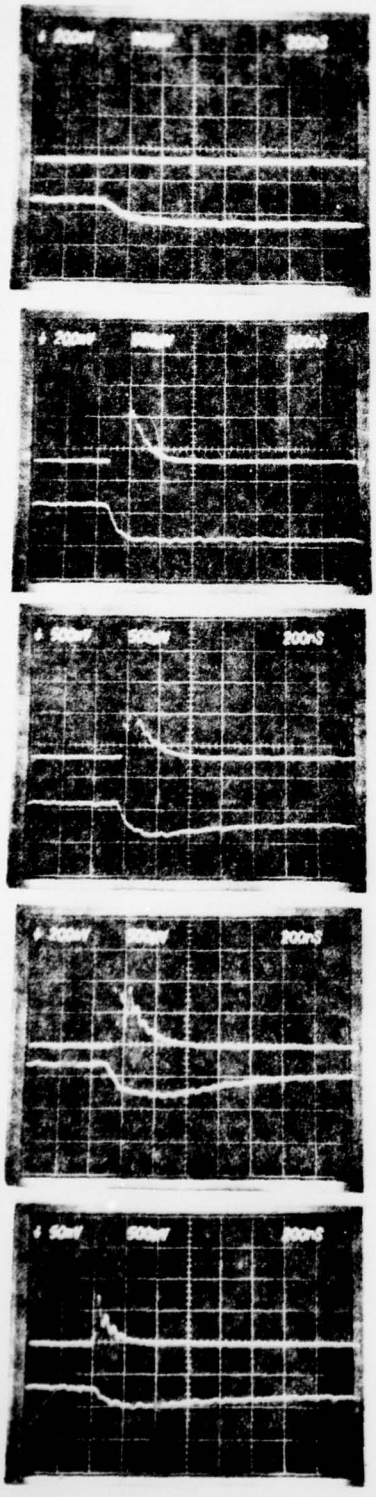

5–5

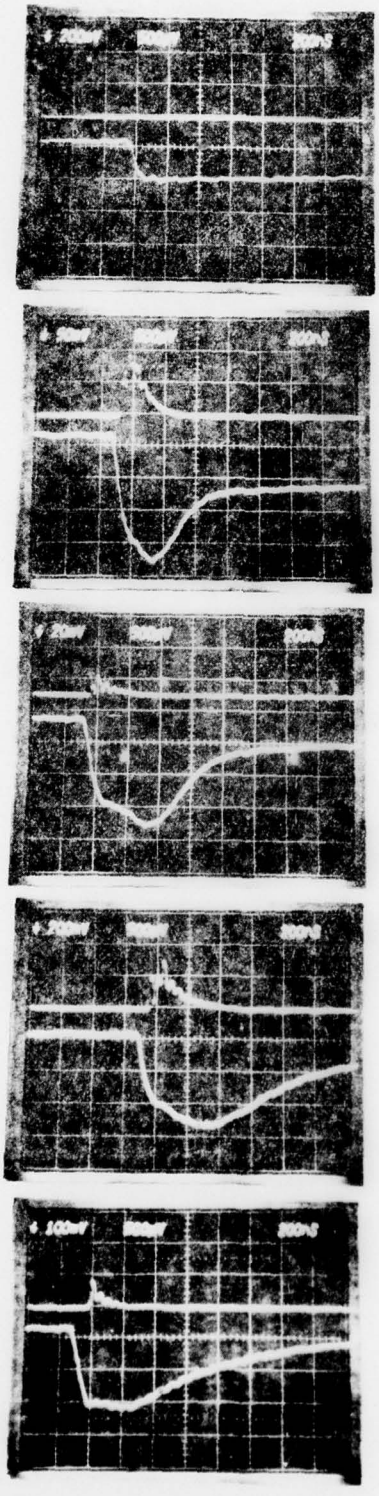

5–6

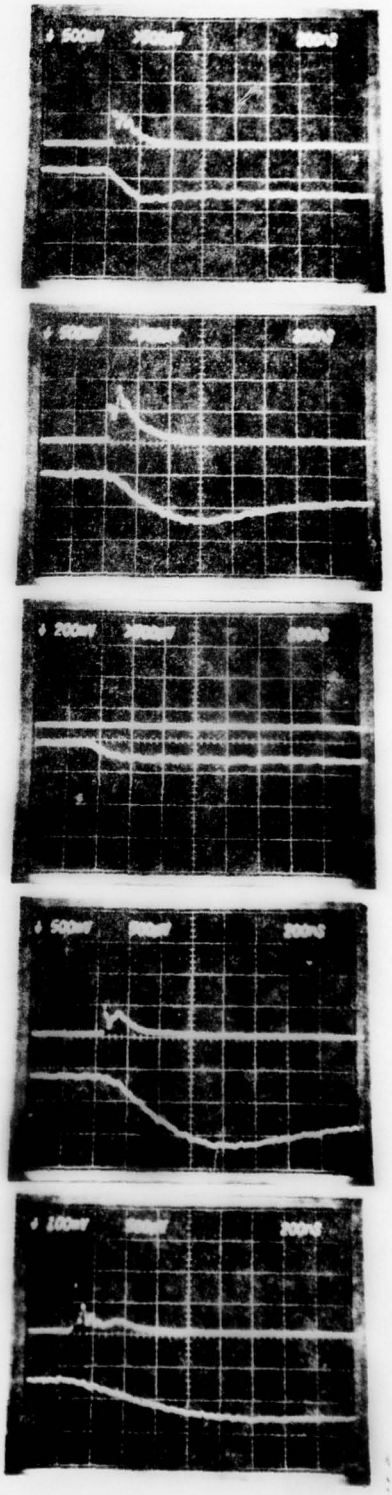

FIG. 21

V–R POPULATION TRANSFER

FROM V = 1, J = 3 TO V = 0, J = 8

1.0 TORR

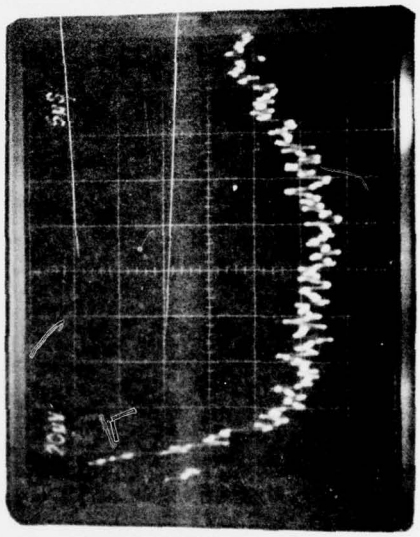

FIG. 22

DECAY OF HF (J=3) POPULATION

(37m TORR)

A

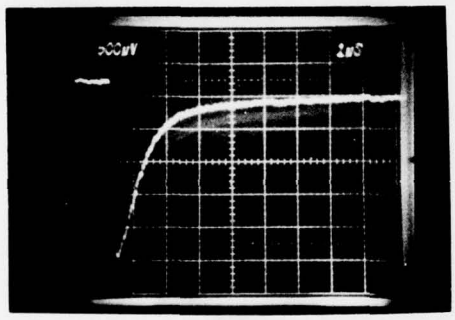

B